ISSN 2320-2092

International Journal of Mechanical & Production Engineering (IJMPE)

Volume No. 13
Issue No. 2
May- August 2025

ENRICHED PUBLICATIONS PVT. LTD

S-9, IInd FLOOR, MLU POCKET,
MANISH ABHINAV PLAZA-II, ABOVE FEDERAL BANK,
PLOT NO-5, SECTOR-5, DWARKA, NEW DELHI, INDIA-110075,
PHONE: - + (91)-(11)-47026006

ISSN 2320-2092

International Journal of Mechanical & Production Engineering (IJMPE)

Aim & Scope

The International Journal of Mechanical & Production Engineering (IJMPE) is an international forum for the publication and dissemination of original work which contributes to greater scientific understanding of the main disciplines underpinning the whole spectrum of mechanical engineering, which includes, but is not limited to, Materials and Design Engineering, Production Engineering and Fusion Technology, Dynamics, Vibration and Control, Thermal Engineering and Fluids Engineering, Environmental protection, etc..

The IJMPE is a peer-reviewed open access journal published monthly in English-language. Only original, innovative and novel papers will be considered for publication in the International Journal of Mechanical Sciences and before considering their work, authors are required to confirm that their paper has not been submitted to any other journal in English or any other language. Original ideas may be discussed in advance with the Editor (mail: Info.Ijmpe@Gmail.Com), to clear the ground for a draft submission. All papers are then peer reviewed by relevant experts and feedback is given whether or not a paper is accepted or returned for further work. The Editor's policy is to try and accommodate contributions of all sizes above the minimum threshold where length is dictated by the needs of the subject matter.

The Journal can be found from the official URL www.ijmpe.iraj.in

ISSN 2320-2092

Chief Editor

Editor

Associate Editor

Managing Editor

Editorial Board

ISSN 2320-2092

ISSN 2320-2092

International Journal of Mechanical & Production Engineering (IJMPE)

(Volume No. 13, Issue No. 2, May- August 2025)

Contents

ISSN 2320-2092

ISSN 2320-2092

FINITE ELEMENT ANALYSIS ON FORCED CONVECTIVE HEAT TRANSFER AUGMENTATION OF NANOFLUIDS IN A TRIANGULAR CAVITY

1M.M.BILLAH, 2U.K.SUMA, 3M.M. RAHMAN, 4AZHARUL KARIM
1Department of Arts and Sciences, Ahsanullah University of Science and Technology, Dhaka, Bangladesh
2Department of Mathematics, Bangladesh University, Dhaka, Bangladesh
3Department of Mathematics, Bangladesh University of Engineering and Technology, Dhaka, Bangladesh

ABSTRACT

The behavior of Ag-water nanofluids is explored numerically in an inclined lid-driven triangular enclosure heated on bottom surface. The consequent mathematical model is governed by the coupled equations of mass, momentum and energy and solved by employing Galerkin weighted residual method of finite element formulation. A wide range of governing parameters such as the Richardson number and Reynolds number are considered in this investigation. Ag-water nanofluids are used with Prandtl number, Pr = 6.2 and Reynolds number (Re) is varied from 100 to 500.The streamlines, isotherm plots and the variation of the average Nusselt number at the hot surface as well as average fluid temperature in the enclosure is presented and discussed in detailed. It is observed that Reynolds number strongly influenced the fluid flow and heat transfer in the enclosure at the three convective regimes.

Keywords *- Ag-water nanofluid, Finite Element Method, solid volume fraction*

I. INTRODUCTION

Nanofluids come out to have a very high thermal conductivity which can meet the intensifying demand as an efficient heat transfer agent. Researchers have started showing interest in the study of heat transfer characteristics of these nanofluids in recent years. A prodigious importance has been shown to the forced convection heat transfer phenomena as it has a very wide range of application in heat exchangers, solar collector, electronics cooling, desalination process and so on The convective heat transfer feature of nanofluids is influenced by the thermo-physical properties of the base fluid and nano particles. The function of a meticulous nanofluid for a heat-transfer intention can be traditional by properly modeling the convective transportation in the nanofluid [1]. A numerical study is performed to analyze the transport mechanism of mixed convection in a lid-driven enclosure packed with nanofluids by Muthtamilselvan et al. [2]. Sheikholeslami et al. [3] conducted the forced
convection heat transfer in a semi annulus under the influence of a variable magnetic field using ferrofluid (Fe3O4). They found that the effects of Kelvin forces are more pronounced for high Reynolds number and heat transfer enhancement has direct relationship with the Reynolds number. A parametric study on mixed convection flow in a lid-driven inclined square enclosure filled with water-Al2O3 nanofluid was performed by Nada and Chamkha [4]. Mansour et al. [5] conducted a numerical simulation on mixed convection flow in a square lid-driven cavity partially heated from below using nanofluid. Eastman et al. [6] considered pure copper nanoparticles of less than 10 nm sized and achieved 40% increase in thermal conductivity for only 0.3% volume fraction of the solid dispersed in ethylene glycol. Tzeng et al. [7] investigated the effect of nanofluids when used as engine coolants. CuO and

Al2O3 and antifoam were individually mixed with automatic transmission oil. In this study, the effect of Reynolds number is investigated numerically.

II. PROBLEM ANALYSIS

A. Physical Configuration

The physical model is depicted in Fig. 1. The problem deals with a steady two-dimensional flow of nanofluid contained in an inclined lid-driven triangular enclosure. The length of the base wall and height of the sliding wall of the enclosure are considered by L and H, respectively. In addition, the sliding wall of the cavity is kept adiabatic and allowed to move from bottom to top at a constant speed V0. Moreover, it is assumed that the temperature (Th) of the heating part of the bottom wall is higher than the temperature (Tc) of the right inclined wall.

B. Thermo physical property of nanofluid

The nanoparticles of Ag are assumed to have a uniform shape and size. Furthermore, it is assumed that both the fluid phase and nanoparticles are in thermal equilibrium state and they flow at the same velocity. The thermo physical properties of the nanofluid are assumed to be constant except for the density variation in the buoyancy force, which is based on the Boussinesq approximation. The data used for the numerical simulation [8] is given in Table1.

C. Mathematical Modeling

The free space in the enclosure is filled with Ag-water nanofluids. The nanofluid in the enclosure I Newtonian, incompressible and laminar. The nanoparticles are assumed to have uniform shape and size. Under the above assumptions, the system of equations governing the two-dimensional motion of a nanofluid is as follows:

$$\frac{\partial u}{\partial x}+\frac{\partial v}{\partial y}=0 \tag{1}$$

$$u\frac{\partial u}{\partial x}+v\frac{\partial u}{\partial y}=-\frac{1}{\rho_{nf}}\frac{\partial p}{\partial x}+\frac{\mu_{nf}}{\rho_{nf}}\left(\frac{\partial^2 u}{\partial x^2}+\frac{\partial^2 u}{\partial y^2}\right)+\frac{(\rho\beta)_{nf}}{\rho_{nf}}(T-T_c)g\sin\phi \tag{2}$$

$$u\frac{\partial v}{\partial x}+v\frac{\partial v}{\partial y}=-\frac{1}{\rho_{nf}}\frac{\partial p}{\partial y}+\frac{\mu_{nf}}{\rho_{nf}}\left(\frac{\partial^2 v}{\partial x^2}+\frac{\partial^2 v}{\partial y^2}\right)+\frac{(\rho\beta)_{nf}}{\rho_{nf}}(T-T_c)g\cos\phi \tag{3}$$

$$u\frac{\partial T}{\partial x}+v\frac{\partial T}{\partial y}=\alpha_{nf}\left(\frac{\partial^2 T}{\partial x^2}+\frac{\partial^2 T}{\partial y^2}\right) \tag{4}$$

The effective density of the nanofluid is defined by

$$\rho_{nf}=(1-\delta)\rho_f+\delta\rho_s \tag{5}$$

where δ is the solid volume fraction of nanoparticles. The thermal diffusivity of the nanofluid is defined as:

$$\alpha_{nf} = \frac{k_{nf}}{(\rho c_p)_{nf}} \quad (6)$$

The heat capacitance of nanofluids can be defined as:

$$(\rho c_p)_{nf} = (1-\delta)(\rho c_p)_f + \delta(\rho c_p)_s \quad (7)$$

The thermal expansion coefficient of the nanofluid can be defined by

$$(\rho\beta)_{nf} = (1-\delta)(\rho\beta)_f + \delta(\rho\beta)_s \quad (8)$$

The dynamic viscosity of the nanofluid is defined as:

$$\mu_{nf} = \frac{\mu_f}{(1-\delta)^{2.5}} \quad (9)$$

The effective thermal conductivity of nanofluid was intoduced as:

$$\frac{k_{nf}}{k_f} = \frac{k_s + 2k_f - 2\delta(k_f - k_s)}{k_s + 2k_f + \delta(k_f - k_s)} \quad (10)$$

where, ks is the thermal conductivity of the nanoparticles and kf is the thermal conductivity of base fluid. Introducing the following dimensionless variables

$$X = \frac{x}{L}, Y = \frac{y}{L}, U = \frac{u}{V_0}, V = \frac{v}{V_0},$$
$$P = \frac{(p + \rho g y)L^2}{\rho_{nf} {V_0}^2}, \theta = \frac{(T - T_c)}{(T_h - T_c)} \quad (11)$$

the governing equations may be written in the dimensionless form as

$$\frac{\partial U}{\partial X} + \frac{\partial V}{\partial Y} = 0 \quad (12)$$

$$U\frac{\partial U}{\partial X} + V\frac{\partial U}{\partial Y} = -\frac{\partial P}{\partial X} + \frac{1}{Re}\frac{\rho_f}{\rho_{nf}}\frac{1}{(1-\delta)^{2.5}}\left(\frac{\partial^2 U}{\partial X^2} + \frac{\partial^2 U}{\partial Y^2}\right) + \frac{(\rho\beta)_{nf}}{\rho_{nf}\beta_f} Ri\theta\sin\phi \quad (13)$$

$$U\frac{\partial V}{\partial X} + V\frac{\partial V}{\partial Y} = -\frac{\partial P}{\partial Y} + \frac{1}{Re}\frac{\rho_f}{\rho_{nf}}\frac{1}{(1-\delta)^{2.5}}\left(\frac{\partial^2 V}{\partial X^2} + \frac{\partial^2 V}{\partial Y^2}\right) + \frac{(\rho\beta)_{nf}}{\rho_{nf}\beta_f} Ri\theta\cos\phi \quad (14)$$

$$U\frac{\partial \theta}{\partial X} + V\frac{\partial \theta}{\partial Y} = \frac{\alpha_{nf}}{\alpha_f}\frac{1}{Re\,Pr}\left(\frac{\partial^2 \theta}{\partial X^2} + \frac{\partial^2 \theta}{\partial Y^2}\right) \quad (15)$$

The nondimensional numbers that appear in equations (13) -(15) are as follows:

Reynolds number $Re = V_0 L/\upsilon_f$, Prandtl number $Pr = \nu_f/\alpha_f$ and Richardson number $Ri = g\beta_f (T_h - T_c) L/V_0^2$

The appropriate boundary conditions for the governing equations are

on the bottom wall: $U = V = 0, \theta = 1$ (on the heater), $U = V = 0, \frac{\partial \theta}{\partial N} = 0$ (on the unheated part)

on the left inclined wall: $U = 0, V = 1, \frac{\partial \theta}{\partial N} = 0$

on the right inclined wall: $U = V = 0, \theta = 0$

where N is the non-dimensional distances either X or Y direction acting normal to the surface.The average Nusselt number at the heated surface of the cavity may be expressed as

$$Nu_{av} = -\frac{k_{nf}}{k_f}\int_0^1 \frac{\partial \theta}{\partial Y} dX \quad (16)$$

and average fluid temperature in the enclosure may be defined as $\Theta = \int \theta d\overline{V}/\overline{V}$ (17)

III. COMPUTATIONAL DETAILS

We use the Galerkin weighted residual method of finite element formulation as a computational scheme. The finite element method begins by the partition of the continuum area of interest into a number of simply shaped regions known as elements. These elements may be different shapes and sizes. Within each element, the dependent variables are approximated using interpolation functions. In the present study, erratic grid size system is considered especially near the walls to capture the rapid changes in the dependent variables. The coupled governing equations (12)-(15) are transformed into sets of algebraic equations using finite element method to reduce the continuum domain into discrete triangular domains. The system of algebraic equations is solved by iteration technique. The solution process is iterated until the subsequent convergence condition is satisfied: $\left|\Gamma^{m+1} - \Gamma^m\right| \le 10^{-6}$ where m is number of iteration and Γ is the general dependent variable.

Table 1. Thermophysical properties of water and nanoparticles [8]

Properties	water	Ag
c_p	4179	235
ρ	997.1	10500
k	0.613	429
β	2.1×10^{-4}	5.4×10^{-5}

IV. RESULTS AND DISCUSSION

In this study, our attention is taken into account to investigate the effects of controlling parameters namely the Reynolds number and Richardson number (Ri). Here, solid volume fraction (δ) and tilt angle are kept fixed at 4% and 60, respectively.

The effect of Reynolds Number Re and Ri on the fluid flow and temperature distribution in the cavity are illustrated in the Figs.2 and 3 by plotting the streamlines and isotherms for Re = 100, 200, 300 and 500 and various Ri (0, 1 and 10), while δ = 0.04 and = 60o. The basic flow structure in the absence of natural convection effect is presented in the left bottom corner of Fig. 2 at Re = 100. It is seen clearly that for Ri = 0.1 and low Reynolds number (Re = 100), the forced convection plays a dominant role, and the recirculation flow is mostly generated only by the moving lid. The fluid flow in a two dimensional lid-driven triangular enclosure is characterized by a main circulating cell (major cell) near the vicinity of the sliding left surface in the enclosure developed by the lid and a weaker anticlockwise rotating cell close to the right bottom corner for all values of Re. It can easily be seen the left column of Fig.2, the key cell is created by the lid exhausted the neighboring fluid. In addition, the flow strength and the size of the key cell is decreases with the increasing values of Re. On the other hand, it is found from the streamlines that the flow strength as well as the size of the anticlockwise rotating cell escalating very moderately when Re is increased. With increment in Re at Ri = 1, buoyancy driven becomes stronger than the vortex due to the moving lid. Finally, for Ri = 10 and different values of Re (= 100, 200, 300 and 500) the flow patterns are characterized by two asymmetrical vortices that occupy the entire cavity as reflected in the column of the Fig. 2. It is noticed that most of the part of the cavity is covered by the minor cell. It also seems that the mechanical effect generated by the moving lid
is dominated by the buoyancy forces.

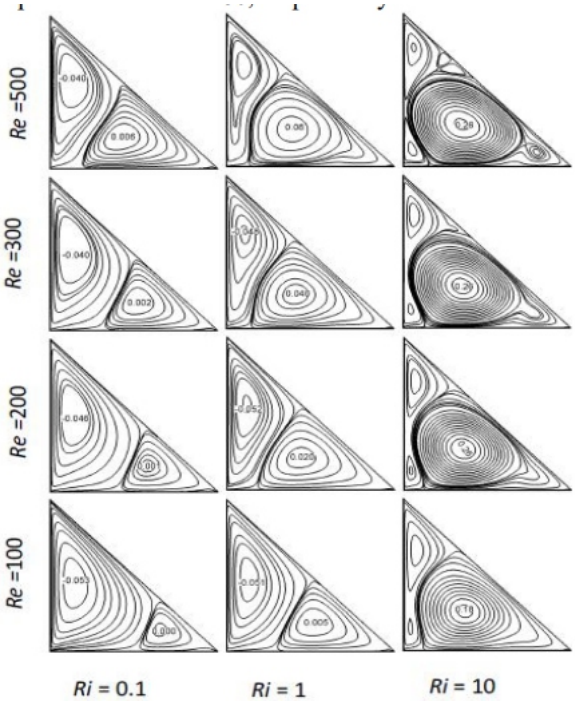

Fig.2 Streamlines for different values of Reynolds number Re and Richardson number Ri.

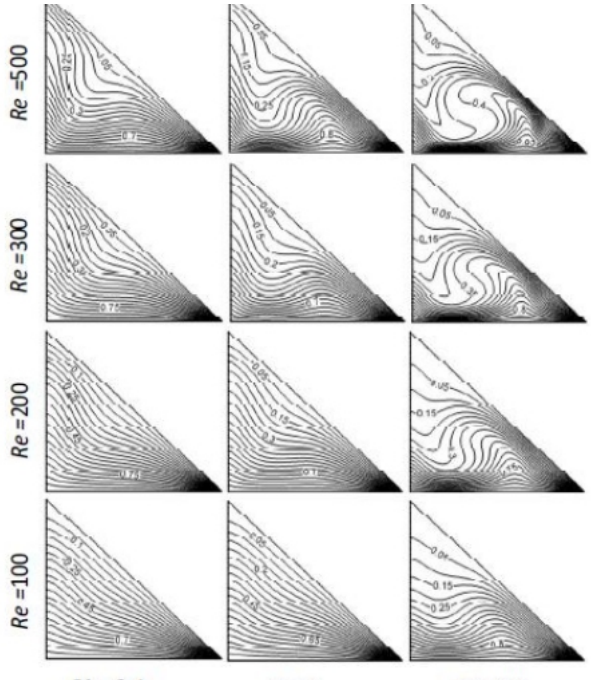

Fig.3 Isotherms for different values of Reynolds number Re and Richardson number Ri.

The corresponding isotherm patterns for different Reynolds number and Richardson number at δ = 0.04 are displayed in Fig.3. From the left column of this figure, it is seen that the isotherms for different values of Re at Ri = 0.1 are clustered near the heated surface of the enclosure, which indicates a steep temperature gradient along the horizontal direction in this region. Moreover, in the remaining area of the cavity, the temperature gradients are very small due to the mechanically-driven circulations.
Additional, at Ri = 1, the thermal layer near the hot surface becomes thin and wavy isotherms observed for higher Re. Which indicates the steeper thermal gradient becomes strong with escalating Re.

Furthermore, as Ri increases to 10 the thermal layernear the hot surface become very thin and the thermal spot is developed between the two rotating cells.

The average Nusselt number at the heat source is plotted as a function of Richardson number for a particular Reynolds number is revealed in Fig. 4. Fig.4presents a very instructive picture of how the heat is transferred in accordance with Re and Ri. The average Nusselt number at the heated surface decreases very swiftly for higher values of Re with increasing value of Ri up to mixed convection regime but it increases for higher values of Re with increasing value of Ri >0. On the other hand, the average Nusselt number at the heated surface remains constant for lower value of Re (= 100) with increasing value of Ri up to mixed convection regime, later it increases. However, the average Nusselt number at the heated surface is found to increase as Re increases at fixed Ri. These results are probable because nanoparticles increases heat absorbing capacity of the base fluid. Therefore, it can be concluded that more heat transfer from the heat source is expected in the case of large parameter value of Re or Ri. One can notice that the values of Nu are lower for the pure mixed convection (Ri = 1), while it compared with that for the other values of Ri. Nevertheless, the values of Nuav are always maximum for the higher value of Re (= 500).

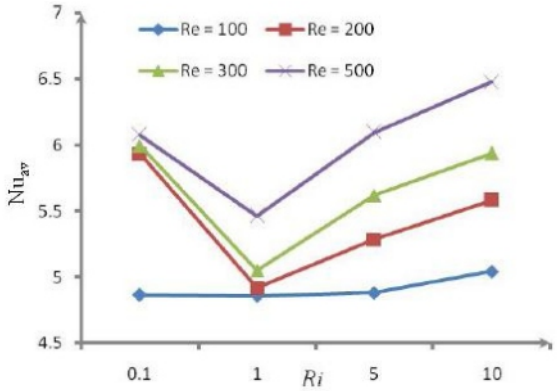

Fig. 4 Effect of Reynolds number Re on average Nusselt number at the heated surface in the cavity.

The effect of Reynolds number Re on average fluid temperature θav in the cavity is revealed in the Fig. 5. From this figure, it can clearly be seen that the value of θav decreases promptly with the raise of Ri for all considered Reynolds number. However, the values of Nuav are always maximum for the lower value of Re (= 100).

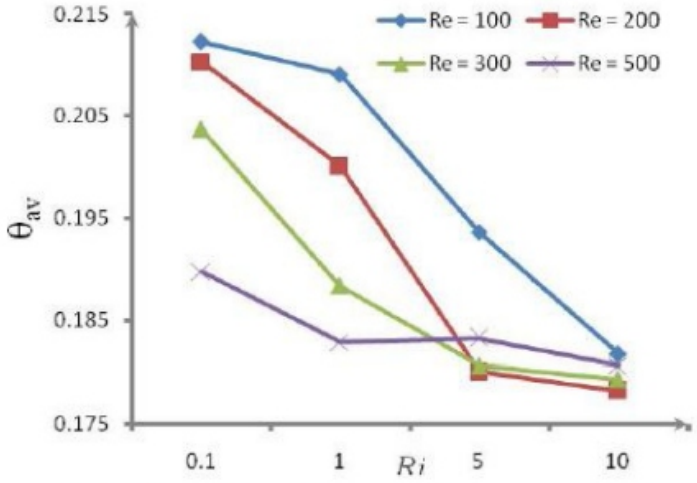

Fig.5. Effect of Reynolds number Re on average fluid temperature in the cavity.

CONCULISION

Forced convection parameter Re has a great significant effect on the streamlines and isotherms field. Buoyancy-induced vortex in the streamlines increased and thermal layer near the heated surface become thin and concentrated with increasing Re. In addition, the heat transfer increased by roughly 14.46% at Ri =1 but it increased by about 30.28.35% at Ri =10 as Re increases from100 to 500. The average Nusselt numbers at the heated surface is always upper and average temperature in the cavity is inferior for the large value of Re. Moreover, Ag-water nanofluids are capable to modify the flow pattern. The solid volume fraction is a good control parameter for both pure and nanofluid filled enclosures.

ACKNOWLEDGEMENT

The work is supported by Ahsanullah University of Science and Technology.

REFERENCES

[1] R. Saidur, S.N. Kazi, M.S. Hossain, M.M. Rahman, H.A. Mohammed, "A review on the performance of nanoparticles suspended with refrigerants and lubricating oils in refrigeration systems", Renewable and Sustainable Energy Reviews, vol. 15 pp. 310–323, 2011.

[2] M. Muthtamilselvan, P. Kandaswamy, J. Lee, "Heat transfer enhancement of copper-water nanofluids in a lid-driven enclosure", Commun. Nonlinear Sci Numer Simulat, vol. 15, pp. 1501-1510, 2010.

[3] M. Sheikholeslami, K. Vajravelu, M.M. Rashidi, "Forced convection heat transfer in a semi annulus under the influence of a variable magnetic field", Int. J. of Heat and Mass Transfer, vol. 92, pp. 339-348, January 2016.

[4] E.A. Nada, A.J. Chamkha, "Mixed convection flow in a lid-driven inclined square enclosure filled with a nanofluid", European J. Mechanics B/Fluids, vol. 29, pp. 472-482, 2010.

[5] M.A. Mansour, R.A. Mohamed, M.M. Abd-Elaziz, S.E. Ahmed, "Numerical simulation of mixed convection flows in a square lid-driven cavity partially heated from below using nanofluid", Int. Commun. Heat Mass Transfer, vol. 37, pp.1504–1512, 2010.

[6] J.A. Eastman, S. U. S. Choi, S .Li, W. Yu, and L. J. Thompson, "Anomalously increased effective thermal conductivities of ethylene glycol-based nanofluids containing copper nanoparticles", Appl Phys Lett, vol. 78, pp. 718-20, 2001.

[7] S.C. Tzeng, C.W. Lin, K.D. Huang, "Heat transfer enhancement of nanofluids in rotary blade coupling of four-wheel-drive vehicles", Acta Mechanica, vol. 179, pp.11-23, 2005.

[8] Sameh E. Ahmed, M.A. Mansour, A.K. Hussein, S. Sivasankaran, "Mixed convection from a discrete heat source in enclosures with two adjacent moving walls and filled with micropolar nanofluids," Engineering Science and Technology, an International Journal, vol. 19, pp.364-376, 2016.

ISSN 2320-2092

GRAIN REFINEMENT OF CAST AL-SI-MG ALLOYS USING ELECTROMAGNETIC STIRRING

1A. K. RAJAK, 2B. B. KUMAR, 3C. K. MEENA, 4D. K. DWIVEDI
1Department of Mechanical & Industrial Engineering, Indian Institute of Technology, Roorkee, India

A B S T R A C T

This paper describes the effect of electromagnetic stirring current (11-15A) on the microstructure of Al-7%Si 0.5%Mg and Al-17%Si-0.5%Mg alloys. Electromagnetic stirring (EMS) of semi-solid aluminium alloys was carried out under continuous cooling conditions. To investigate the effectiveness of the EMS systems, castings processed by EMS using different current values and mechanical stirring were prepared using graphite mould (to ensure slow cooling rate). It was found that EMS can be effectively used with hypoeutectic and hypoeutectic Al-Si alloys to get modified eutectic even without any modifier. EMS was found to be more effective than mechanical stirring in controlling the microstructure of as cast samples. The optimum current for EMS to achieve the better control over the structure varies with silicon content in the alloy. Optimum current was found to increase with increase in Si content in aluminium alloy. At very low currents the Electromagnetic stirring gave better results as compared to that at high current and mechanical stirring. Results were substantiated by scanning electron microscopy

Keywords *- Cast Al-Si-Mg alloy, electromagnetic stirring, mechanical stirring, current, eutectic modifications and grain*

I. INTRODUCTION

Application of aluminium in automotive and aerospace is increasing continuously due to some very attractive characteristics like high strength to weight ratio, good wear and corrosion resistance and easy to process. These factors in turn help inproducing the light weight and energy vehicle with less emission gases (CO2 and No2). Conventional liquid metal casting processes face many potential problems such as gas entrapment, hot tearing, and shrinkage porosity formation. Hot tearing occurs due to low ductility and poor strength of dendritic network in the semi-solid state during the solidification, while formation of shrinkage porosity is attributed to poor feeding of liquid metal through the dendritic network. Therefore, most of the research worldwide has been concentrated on the refinement and development of non-dendritic morphologies in hypoeutectic and hypereutectic Al-Si alloys to overcome these problems of conventional liquid casting processes. It has been suggested that problems can be greatly reduced by having spheroidal primary phase morphologies [1]. Controlling the rheology of the semi- solid metal (SSM) slurries is one of ways to achieve spheroidal solid morphology. Rheocasting began at MIT in 1971 to produce non-dendritic microstructures by continuous stirring of solidifying metal through the solidification temperature range [2]. There are basically two approaches to obtain the desired microstructure for a semi-solid slurry using different techniques: 1) partial solidification of melt under forced convection induced by electro-magnetic or mechanical stirring or partial solidification under the effect of external field such as pulse current or ultrasonic vibrations; and 2) partial melting of solid feed stock solidified under controlled conditions.

Though the research on stir-casting picked up in late eighties but literature review reveals that only few references [3-9] are available on improving the structure and mechanical properties of hypoeutectic and

hypereutectic Al-Si alloys. Micro-constituents of Al-Si alloy namely primary and eutectic silicon crystals are known to influence to mechanical and tribological properties.

Electromagnetic stirring (EMS) is a technology in which molten metal (in semi solid condition) is stirred with the help of electromagnetic forces. Molten metal is kept in a vessel (generally cylindrical), around the vessel coils are wrapped. Flow of A.C current through the coils generatesvarying magnetic field, which sets current in molten metal as per Lenz's law of magnetic induction. AC current was controlled with a transformer which in turn controls the magnetic induction intensity of the rotary magnetic field, thus finally affects the rotational velocity of the semi-solid melt [9]. Forced convection of molten metal by Electromagnetic Stirring results in two effects 1) finer particles with a non-dendritic morphology and 2) accelerated crystal growth.

Stirring of semi-solid alloy system breaks the dendrites arms which are formed during normal course of solidification and broken parts of dendriticarms act as nucleant thus grain refinement of alpha aluminium is achieved. With increasing shear rate and intensity of turbulence the particle morphology changes from dendritic to spherical via rosette [7-9]. Electromagnetic stirring have been reported to affect the primary silicon particles (PSPs) morphology in two ways 1) the congregating effect and 2) the refining effect. When the stirring current is high, the congregating effect predominates over refinement effect and therefore PSPs move inwards and congregate to form large blocks owing the occurrence of the centrifugal force field. Relatively weak electromagnetic stirring offers more refining effect on the primary Si particles than the strong electromagnetic stirring. The severe EMS causes more turbulence in the semi-solid metal, which in turn encourage fracture of dendritic arms. The turbulence drags the broken grains to the centre of the ingot where they grow in the form of rosettes or globules (morphology more energetically steady). A greater number of broken grains results in a final smaller average grain size. Literature indicates the best refinement and distribution of micro-constituents is obtained only at an optimum level of EMS current[4]. Dendrite fracture theory is widely accepted as primary mechanism for refinement of alpha aluminium in stir cast Al-Si alloys; however, the mechanism of primary and eutectic silicon refinement is not yet very clearly understood [2, 3]. Therefore, in present research attempts were made to investigate the effect EMS (using different current levels) and mechanical stirring on eutectic and primary silicon particles of a hypoeutectic and a hypereutectic Al-Si alloy.

II. EXPERIMENTAL PROCEDURE

2.1 Development of stir cast alloys

Schematic diagram of EMS system along with main components is shown in Fig. 1. Ceramic wool and asbestos sheet were used for thermal insulation of coils as heat transfer might damage the coil windings. For measuring the temperature of molten metal, alumel-chromel thermo couple (K-type) with digital temperature indicator was used to ensure that stirring is done in the mushy zone. The current and voltage supplied to motor were regulated by a 3 phase Auto transformer for controlled supply of current and voltage according to the rating of the windings. For ensuring safety of windings, the temperature of the windings was also measured continuously during stirring. Suitable electro-magnetic filed was designed and generated for stirring of semi-solid Al-7%Si 0.5%Mg and Al-17%Si-0.5%Mg alloy. Base alloys were first prepared by using Al-50%Si, Al-10%Mg and high purity aluminium with help of an induction furnace. Subsequently, one by one each alloy (1.5kg) was re-melted in the induction furnace for electromagnetic stirring treatment. The molten metal at 750°C was poured in the pre-heated (250º C) graphite crucible. The crucible was then placed in electromagnetic filed. After placing the crucible suitably in electromagnetic field, the current was increased gradually until the rotation starts. The

stirring was then continued at a particular value of current till the molten metal stays in mushy zone under continuous cooling conditions. After stirring, the melt slurry was allowed to cool in graphite crucible kept in still air. On complete solidification, the casting was taken out. EMS was carried out using different conditions as shown in Table I. Mechanical stirring was carried out 200rpm using a system schematically shown in Fig 2. Samples of alloy processed by EMS and mechanical stirring were prepared by machining and standard metallographic polishing procedure for microstructure and hardness study. Polished samples were etched with the Keller's reagent (95% water, HF-1%, HNO3-2.5%, HCl1.5%). Microphotographs of the samples were taken at magnification of 500X using scanning electron microscope (Leo, UK) using and then finally image analysis of all microstructures was done using Materials Plus (Dewinter, India) Image analyzer software

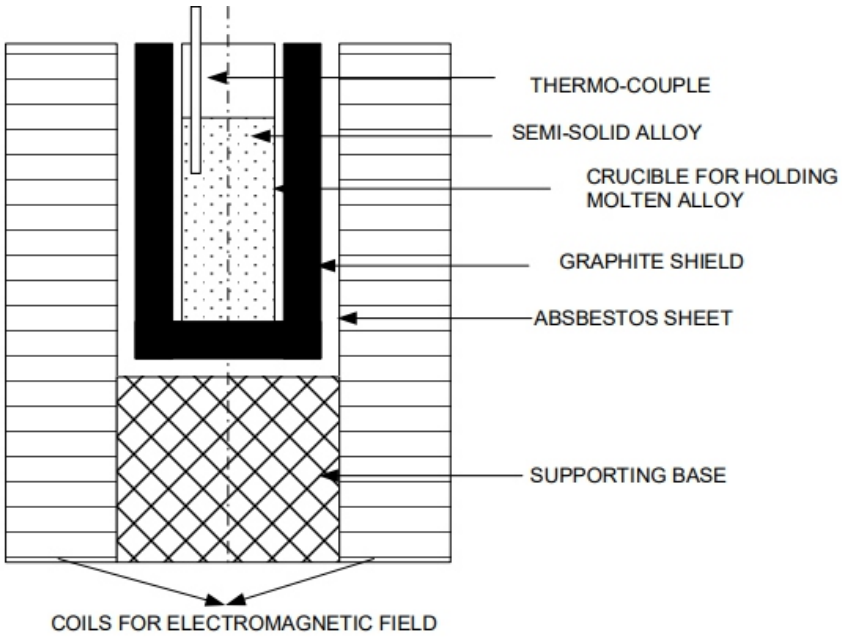

Fig. 1. Schematic diagram of electro magnetic stirring system showing various components

S. No.	Current (A)	Voltage (V)	Temperature Range (°C)	Winding Temp. (°C)
Alloy1	11	150	600-550	41.2
	13	178	-do-	41.8
	15	200	-do-	43.2
Alloy3	11	150	680-600	43.6
	13	178	-do-	44.2
	15	200	-do-	45.4

Table 1: Experimental Parameters for electromagnetic stirring

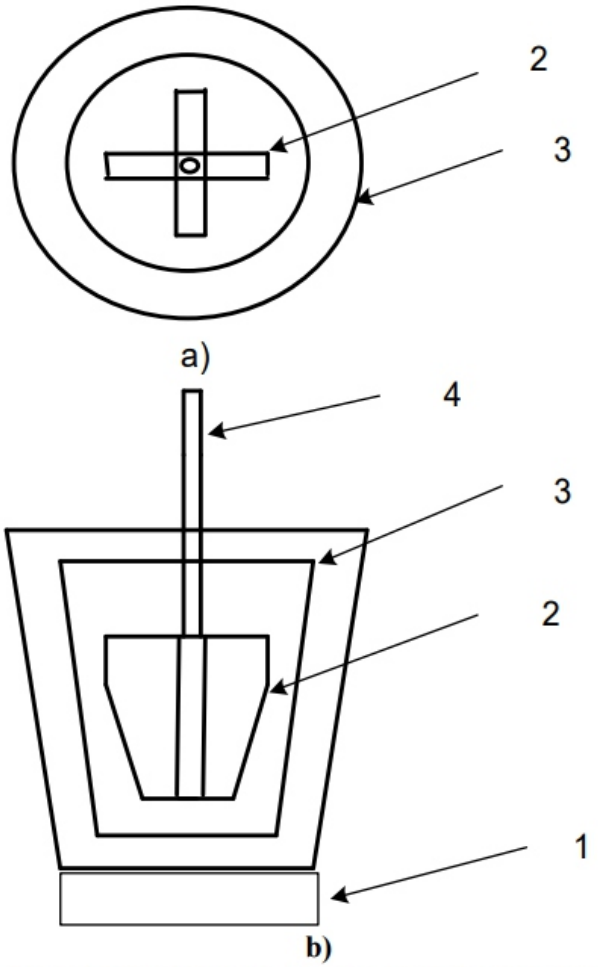

Fig. 2. Schematic diagram of set-up for mechanical stirring showing a) top view and b) front view: 1 hot plate, 2 stainless steel stirrer, 3 graphite crucible and 4 stirrer shaft

III. RESULTS AND DISCUSSION

Microstructures of hypoeutectic alloy processed by EMS and mechanical stirring are shown in Fig. 3 (a d). It can be observed that the microstructure of alloy in different conditions primarily reveal the spheroids, rosettes and eutectic mixture of Al-Si along the grain boundary. In general, increase in EMS current also increases the size of spheroids and coarsens the eutectic mixture especially needle shaped eutectic silicon crystals. Moreover, the EMS of alloy with 11A current results in maximum modification of eutectic and refinement of alpha aluminium grain (Fig 3a). Increase in current from 11A to 15A reduced the degree of modification and grain refinement of the alloy (Fig.3 a-c). Mechanical stirring did not show any major eutectic modification as eutectic silicon remained of needle shape (Fig 3d). This may be due to uniform stirring effect under mechanical stirring conditions.

Microscopy of hypereutectic alloy revealed that EMS at 11A current results is only slight modification of eutectic mixture as many needle shaped silicon particles were observed in matrix of the alloy (Fig 4a). Increase in current from 11 to 13 and 15A caused significant modification of eutectic and refinement of primary silicon particles in the alloy (Fig 4 a-c). Best modification i.e. refinement and spheroidization of eutectic silicon and refinement of primary silicon particles in hypereutectic alloys was observed for sample processed by EMS at 15A current. Mechanical stirring in case of hypereutectic alloy also did not show any significant eutectic modification as eutectic silicon crystals largely remain coarse and needle

shaped (Fig 4 d). Few polyhedral shaped cuboid of primary silicon particles were also observed in alloy matrix.

Morphology of various phases during solidification is governed by growth rate and actual temperature gradient near the solid-liquid metal interface [10-12]. Any kind disturbance in alloy system during solidification affects the stages of solidification i.e. nucleation and growth process. Stirring either using electromagnetic or mechanical (shear) forces leads to fracture of aluminium dendrite growing during the solidification; since the broken dendrites have same composition and crystal structure as that of aluminium, these are able to act as nucleant [10, 11]. Presence of large number of nucleants in semi-solid slurry produced by stirring in turn refines the alpha aluminium grains. Refinement of eutectic modification and primary silicon needs different perception of refinement process. Since aluminium is of higher density (2.84g/cm3) material than silicon (2.4 g/cm3) therefore during stirring under the effect of electromagnetic forces partially solidified aluminium dendrites/grains which are dominating (approx. 80%) in hypoeutectic alloy are churned rigorously which impact onto the eutectic silicon needle and cause their fracture. The extent of fracture of silicon needle during EMS in turn dictates the degree of refinement/modification of eutectic. Once stirring of hypoeutectic alloy is initiated it effectively refines the eutectic and alpha aluminium. In case of hypereutectic alloy, primary silicon particle are nucleated first subsequently eutectic solidifies. Since, silicon is light in weight and non metallic therefore it is does not form dendrite structure but appears as large polyhedral shaped primary silicon which are not broken easily. Stirring of low density coarse cuboid shape primary silicon particle might not be effective at low level of current for electromagnetic stirring which could result in breaking of the silicon needles. This justifies the need of high current for electromagnetic stirring of hypereutectic alloy to achieve the desired refinement/ modification of primary and eutectic silicon particles. Because current directly affects the intensity of magnetic field which in turn affect the electromagnetic forces responsible for stirring of slurry. The magnetic field produced by current carrying coils (solenoid.) is given by

$$B = \mu X N X I$$

Where μ is the magnetic permeability of the material to be stirred, N is number of turns per unit length of

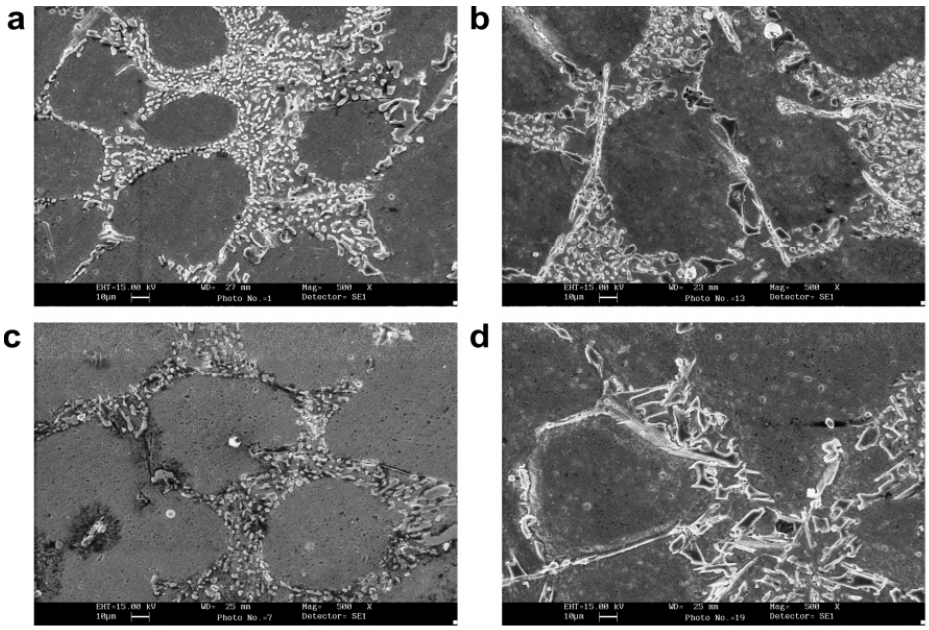

Fig. 3. Effect of stirring on microstructure of hypoeutectic alloy processed by EMS at a) 11A, b) 13A and c) 15A during EMS and d) mechanical stirring

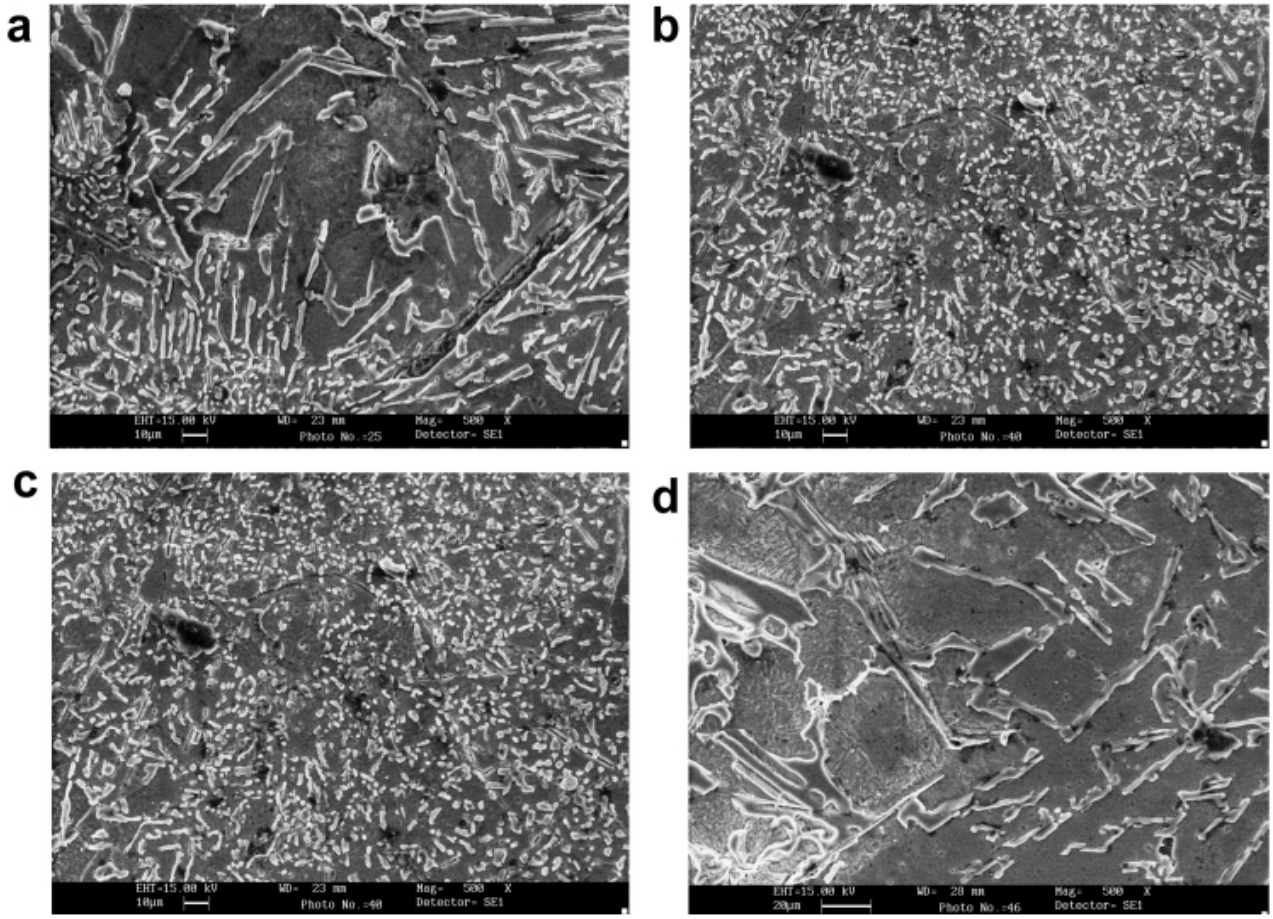

Fig. 4. Effect of stirring on microstructure of hypereutectic alloy at a) 11A, b) 13A and c) 15A during EMS and d) mechanical stirring

the solenoid and I is the current flowing through the coil. Lorentz force on moving charge in a magnetic field is expressed by

$$\vec{F} = e(\vec{v} * \vec{B})$$

Where, e is the charge of electron , v is the velocity of electron, B is magnetic field. The electrons moving in the current loops (eddy current) experience these forces which are held responsible for stirring. The Lorentz force (F) in the metal by an alternating magnetic field, B which induces current density (J), in the metal, and is localized within a certain skin depth.Force F is given by

$$\vec{F} = \vec{J} * \vec{B}$$

Force is normal to the surface of the alloy in the plane of the coil, but decreases with the depth. Occurrence of an optimum level of current for EMS for better control of the microstructure has also been reported earlier however, it was not related to composition or silicon content in the alloy [4].

CONCLUSIONS

1. The electromagnetic stirring (EMS) system was successfully designed and developed for controlling the morphology of alpha aluminium, eutectic and primary silicon particles without any alloying.
2. Electromagnetic stirring of cast hypoeutectic and hypoeutectic Al-Si alloys using different level of currents showed that it can be effectively used to refine and modify the eutectic and primary silicon particles even without any modifier/refiner.
3. Electromagnetic stirring is more effective than mechanical stirring for controlling the microstructure of as cast Al-Si alloys.
4. Optimum current for EMS to achieve the better control over the structure varies with silicon content in the alloy. Optimum current increases with increase in Si percentage.

REFERENCES

[1] G.B. Brook, Improving the Quality of Aluminium Diecastings by Novel Techniques, Fulmer Research Institute, Stoke Poges, Slough SL2 4QD
[2] E.J. Zoqui, M. Paes, E. Es-Sadiqi, Macro and microstructure analysis of SSM A356 produced by electromagnetic stirring, Journal of Materials Processing Technology 120, pp. 365–373, 2002.
[3] W.D. Griffiths, D.G. McCartney, The effect of electromagnetic stirring during solidification on the structure of Al-Si alloys, Materials Science and Engineering A216, pp. 47-60, 1996.
[4] Dehong Lu, Yehua Jiang, Guisheng Guan, Rongfeng Zhou, Zhenhua Li, Rong Zhou, Refinement of primary Si in hypereutectic Al–Si alloy by electromagnetic stirring, Journal of Materials Processing Technology 189, pp. 13–18, 2007.
[5] C. G. Kang, S. W. Youn, Mechanical properties of Particulate Reinforced Metal matrix composites by electromagnetic and mechanical stirring and reheating process for thixoforming, Journal of Materials Processing Technology 147, pp. 10-22, 2004.
[6] B. I. Jung, C.H. Jung, T. K. Han, Y. H. Kim, Electromagnetic stirring and Sr modification in A 356 alloy, Journal of Materials Processing Technology 111, pp. 69-73, 2001.
[7] S. Nafisi, D. Emadi, M. T. Shehata, R. Ghomashchi , Effect of Electromagnetic Stirring & superheat on the microstructural characteristic of Al- Si-Fe alloy, Material Science & Engineering, A 432, pp. 71-83, 2006.
[8] Nancy M, John S. Walker, Strong field electromagnetic stirring in the vertical gradient freeze with submerged heater, Journal of Crystal Growth 291, pp. 249-257, 2006.
[9] Z. Fan, Semisolid Metal Processing, International Material
Reviews, Vol-47, No.2, 2002.
[10] T. V. S. Reddy, D. K. Dwivedi, N. K. Jain, Adhesive Wear of Stir Cast Hypereutectic Al-Si-Mg Alloy Under Reciprocating Sliding Conditions, Wear (accepted).
[11] T V S Reddy, D. K. Dwivedi, N K Jain, Effect of stir-casting on the microstructure and adhesive wear characteristics of cast Al-Si-Cu alloy, Proceeding of IMECHE Journal of Engineering Manufacture (accepted).
[12] D. K. Dwivedi, Ashok Sharma, T V Rajan, Influence of silicon morphology and mechanical properties of piston alloys, Materials and Manufacturing Processes, 20, 5, pp. 777-791, 2005

ISSN 2320-2092

FOCUS RESPONSE AN INNOVATIVE GUIDED WAVE TECHNIQUE FOR SIZING OF CORROSION UNDER INSULATION

MAHDI KHALEGHVERDI, 2MORTEZA KAMALIROOSTA
Tubitak inspection and engineering company

A B S T R A C T

Guided Wave technology developed for detecting metal loss and wall thinning in pipework. It is pulse echo system aimed at testing large volumes of material from a single test point, [1].It is initial application was for detecting corrosion under insulation in petrochemical plant , but it has found widespread use in other inspection situation where pipe or tubes are not accessibl.Unlike the other published paper which concentrate on detection of corrosion, in this paper the concentration is on signals evaluation techniques ''Focus Response" for close estimation of corrosion dimentions. However Guided Wave is known as corrosion monitoring method, by applying Focus Response evaluation techniques, it is possible to obtain details information of suspected features and severity of defects by means of defects extension around circumference of pipe without applying another conventinal technique.

Index Terms *- Guided Wave, Corrosion, Focus response*

I. INTRODUCTION

Guided wave is primarily screening tool. The aim of the inspection is to test long lengths of pipe rapidly with 100% coverage of the pipe wall and to identify areas of corrosion or erosion for further evaluation using other NDT method such as conventional ultrasonic test. The technique is sensitive to metal loss on both the outside and inside of the pipe. It is pulse echo system aimed at testing large volumes of material from a single test point.

This technique involves transmitting ultrasonic Lamb waves along the pipe length. By using this method approximately 50 meter of pipe can be inspected from a single location in the best condition. The system has the ability to inspect the pipe in difficult areas, such as road crossings and insulated pipes or elevated. The technique is especially sensitive for detection of corrosion damage in pipes. This equipment allows a rapid screening of the all pipe; screening tools for fast assessment of large parts of installations, Instead of ultrasonic spot checks.

Lamb waves have the potential of propagating over long distances. This System is an ultrasonic unit that clamps onto the surface of the pipe to be examined and sends a torsional and longitudinal wave along the pipeline. This technique allows detecting locations where a minimum of 5% cross section area has been eroded or corroded away. It is a useful tool for searching corrosion of pipe surfaces at pipe supports, underneath insulation, underground piping,

Guided waves travel across the pipe bends, supports, welds, T-joints, etc but cannot pass across flange joints and end pieces. It also gives qualitative information about defects, as only an UT measurement allows defining how much the thickness reduction in the indicated area has been. Welds cause reflection signals at regular distance, providing reference for sensitivity settings and use to set distance amplitude correction (DAC) curves, seeFig 1.

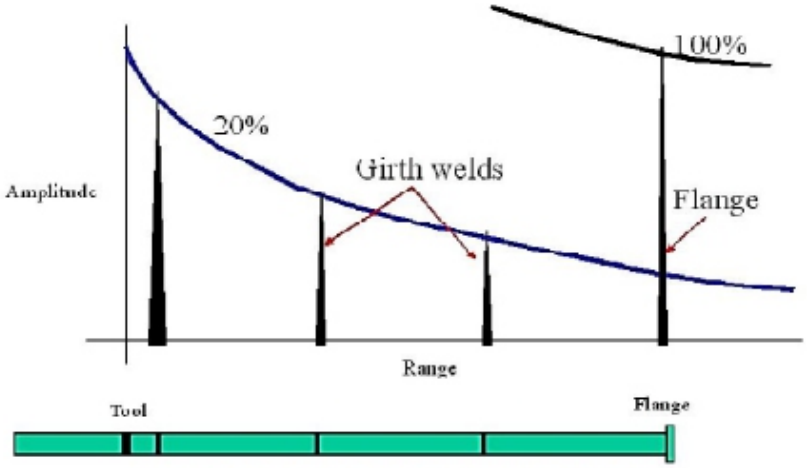

Figure 1:Providing refrence sensitivity

In the case of pipe features such as a girth weld, the increase in thickness is symmetrical around the pipe, so the reflected wave is also symmetrical with same wave mode as the incident wave. In this case we don't have mode conversion signal and this kind of symmetrical signal will show as black color signal in A-scan presentation.see Fig 2 In the case of an area of corrosion, the decrease in thickness is not symmetrical, leading to scattering of the incident wave in addition to reflection the mode conversion also will occur, [3].

The reflected wave will therefore consist of the incident wave mode plus the mode converted components. Therefore this mode converted signal arises from a non-uniform source. This kind of non-uniform signal will present with red or blue color in A-scan presentation. The presence of these signals is a strong indicator of discontinuities such as corrosion, see Fig 3.

A major complication for guided wave system to compare with conventional ultrasonic system is the dispersive nature of guided waves. In the case of dispersion the velocity of most guided waves varies with their frequency, see Fig 4

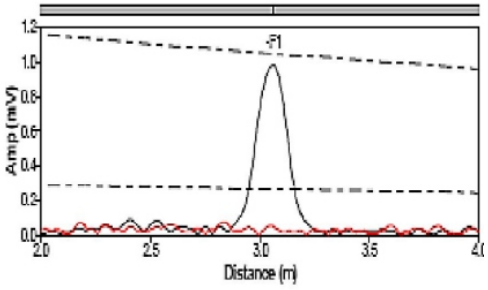

Figure 2: typical weld is symmetric

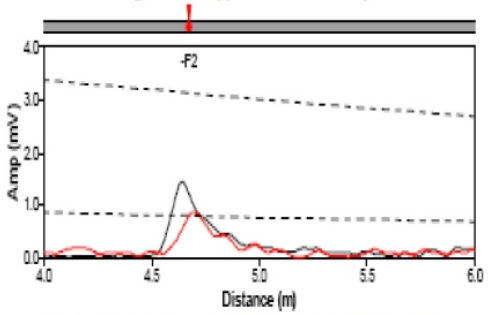

Figure 3: typical corrosion spot is non-symmetric

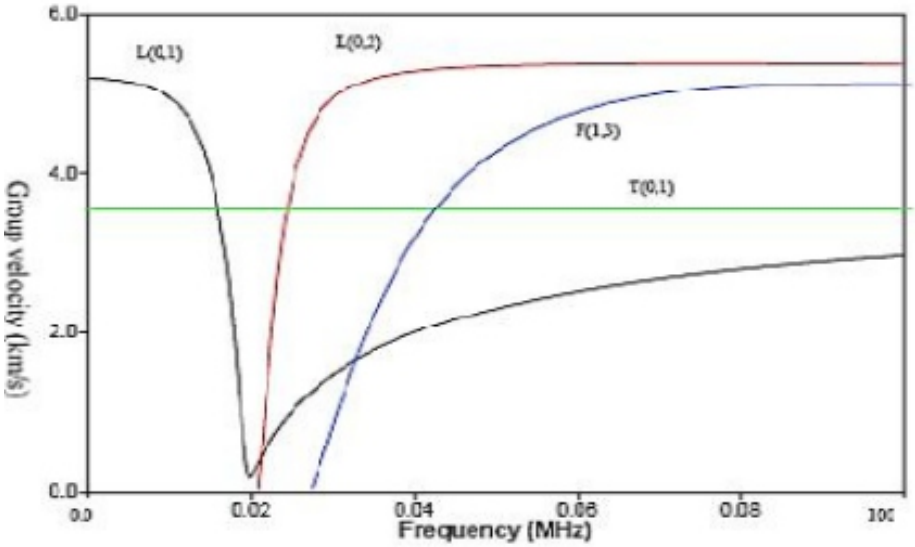

Figure 4: Typical dispersion curves

These are for a specific pipe diameter and wall thickness. Other diameters and thicknesses will have their own families of dispersion curves. It can be seen that the torsional T(0,1) wave is non-dispersive. That is its velocity is constant irrespective of frequency. The L(0,1) wave is highly dispersive with wide variations in velocity with frequency. The L(0,2) wave cannot exist at frequencies below about 20 kHz. These causes major complication to calibrate the time base of the A-scan signals to read as distance and not time. For this purpose the system requires a computer program to read a velocity for the selected test frequency and thickness from a dispersion curve.There is a library of dispersion curves built into the equipment and software for range of pipe diameter/wall-thickness combinations. Tree test locations and also the sketches showing overview of pipe location is shown in Fig 5.

Figure 5: Overview of pipe and examination locations

Presentation of result

For this specific thickness and diameter of the pipe the test frequency has chosen 37 KHz with torsional mode of guided wave in both directions of the pipe.In A-scan plots an additional DAC curves has been added to the analyses screen. This DAC curve will form by connecting the tips of back reflecting signals from welds which are at the same intervals.The A-scan presentation of location one is chosen to show in this paper which is Fig 6. In below of this A-scan, the details of indications involve, type of each indications and distance from datum point is illustrated.

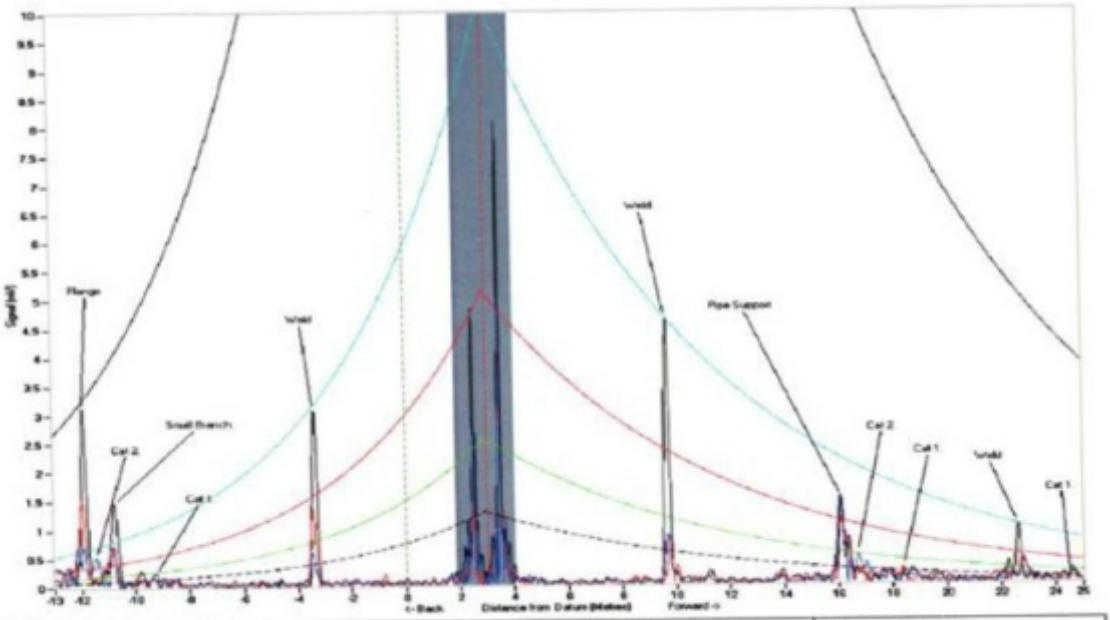

Distance from datum	Indication Type	Comments
-11.691m	Flange	
-11.222m	Cat 2.	Moderate indication
-10.54m	Small Branch	
-9.057m	Cat 1.	Minor indication
-3.143m	Weld	
9.476m	Weld	
15.885m	Pipe Support	Area of Moderate corrosion noted at pipe support
16.478m	Cat 2.	Moderate indication
18.154m	Cat 1.	Minor indication
22.421m	Weld	
24.354m	Cat 1.	Minor indication

Figure 6 : A-scan presentation of location 1

Evaluation techniques

Black & Red Signal technique

The general evaluation technique in all Guided Wave tools is amplitude response directly from red and black signal in A-scan presentation. The black echoes represent from feature that are symmetric around the pipe such as welds and flanges and the red echoes represent from none symmetric feature such as corrosion and supports. The ratio of the red and black signal can be used to approximate the circumferential extent of the observed feature, Fig 7

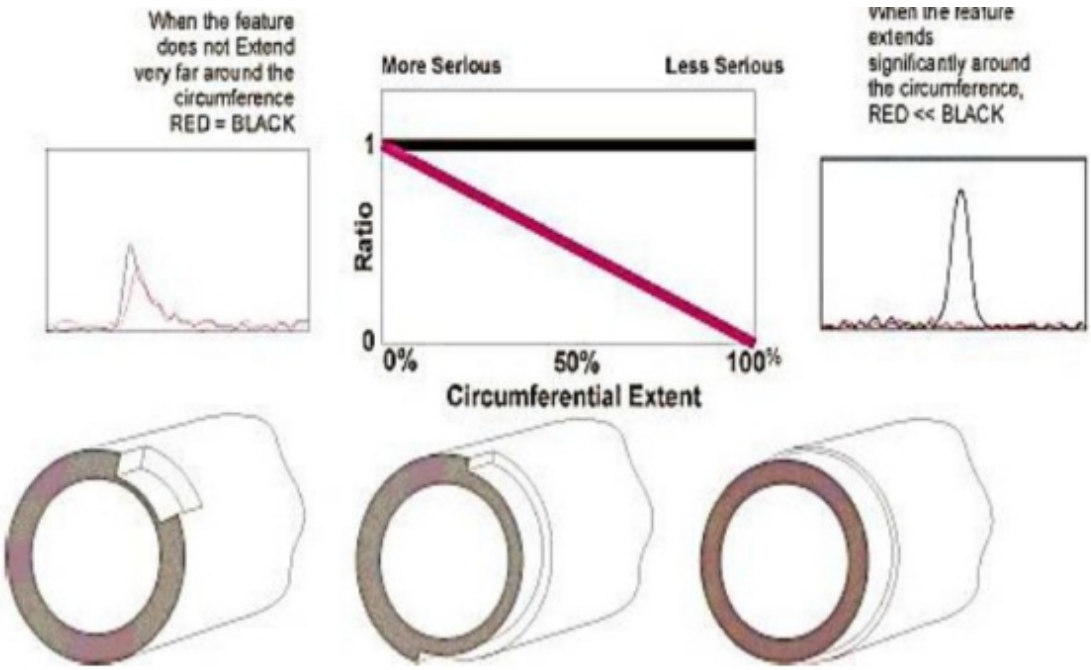

Figure 7: Ratio between red and black signal

Some Guided Wave tools and softwares has ability to send and recive ulrasonic signal during phased delaywhich lead to focus ultrasonic waves in specifc location.By using this specific ability, the focus response technique can be done to get more information of suspected area.

Focus Response technique

Indications identified on the A-scan are evaluated on the basis of a combination of the signal amplitude and directionality of the focused response.In order to provide a means of identifying defect which are potentially significant in terms of the integrity of the pipe , it's also necessary to examine how localized the response around circumference. This may be obtained from the polar response chart.The signal are now describe as being of amplitude category 1,2 or 3, with category 3 being the highest.The additional DAC curve and the areas corresponding to the categories above are shown in Fig 8

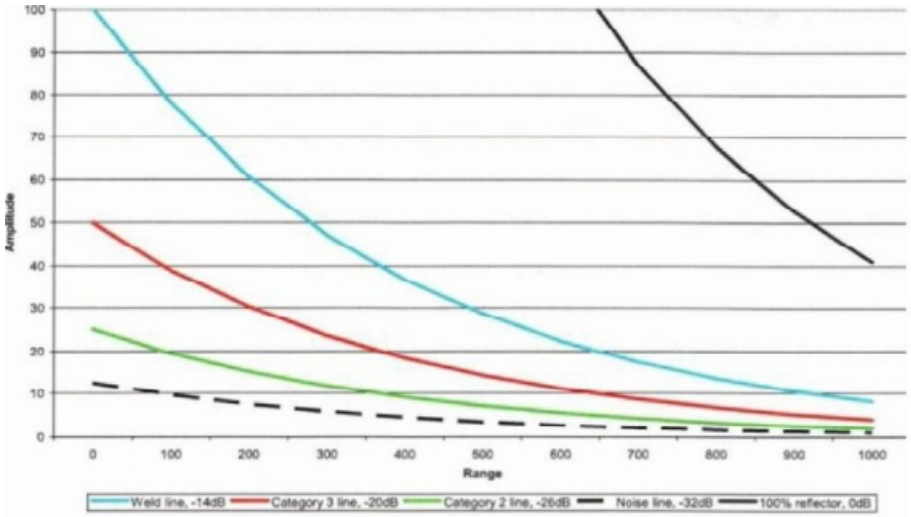

Figure 8: Schematic of amplitude category

Category 1 response is those which are lower than the green -26 db line (formerly Minor).Category 2 response are those above the -26 db line, but are lower than the new red line at -20 db line (Formerly Moderate).Category 3 response exceed the red -20 db line (Formly major).

The collection of focused data from suspected defect is an integral part of the test. The result from focused test on each defect is analyzed in term of the directionality of the response.

If the polar plot shows a high level of directionality , indicated by a single peak in the plot at one focus angle, it classify by category 3, see Fig 9. This indicates that the defect is highly localized on a narrow part of the circumference, so that it is likely to be deep for a given amplitude response.

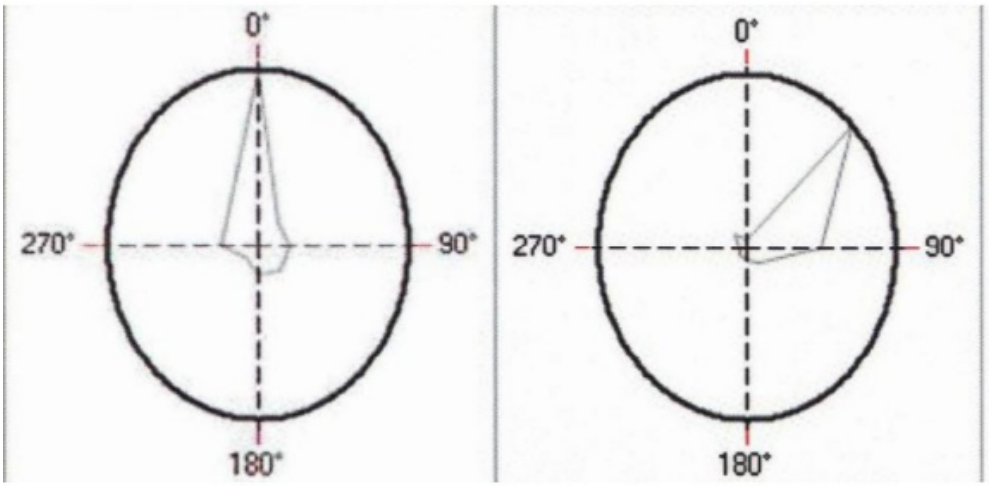

Figure 9: Category 3 response

If the polar plot has two adjacent high amplitude responses it is classify by category 2. This is shown in Fig 10. This suggests that the defect is localized but has some circumferential length.

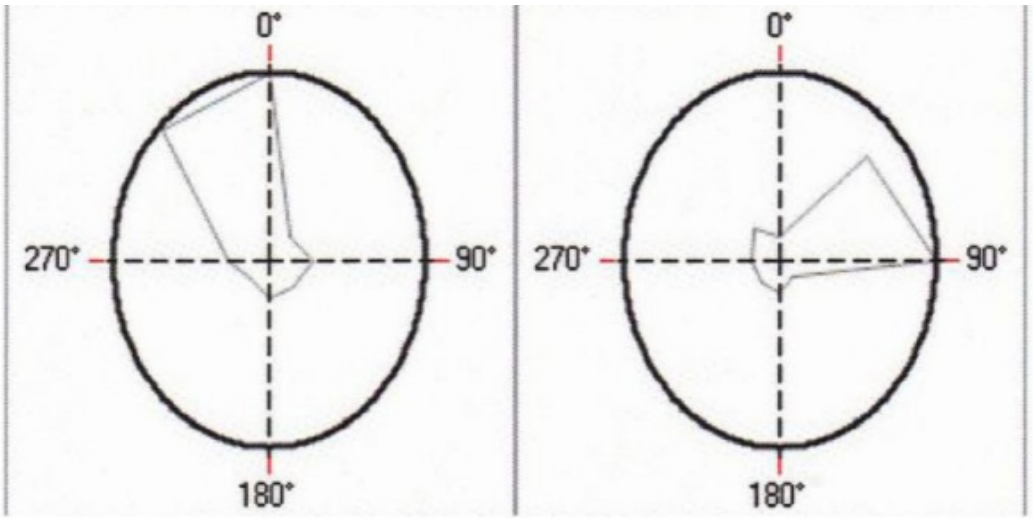

Figure 10: Category 2 response

If the polar plot has 3 or more adjacent high amplitude peaks, see Fig 11it is classify by category 1.This suggests that it is spread over a wide area of circumference, so that it is likely to be less deep for a given response amplitude.Also there is a directionality of category 0, which correspond to the approximately uniform response around the circumference obtained from a weld, see Fig 11

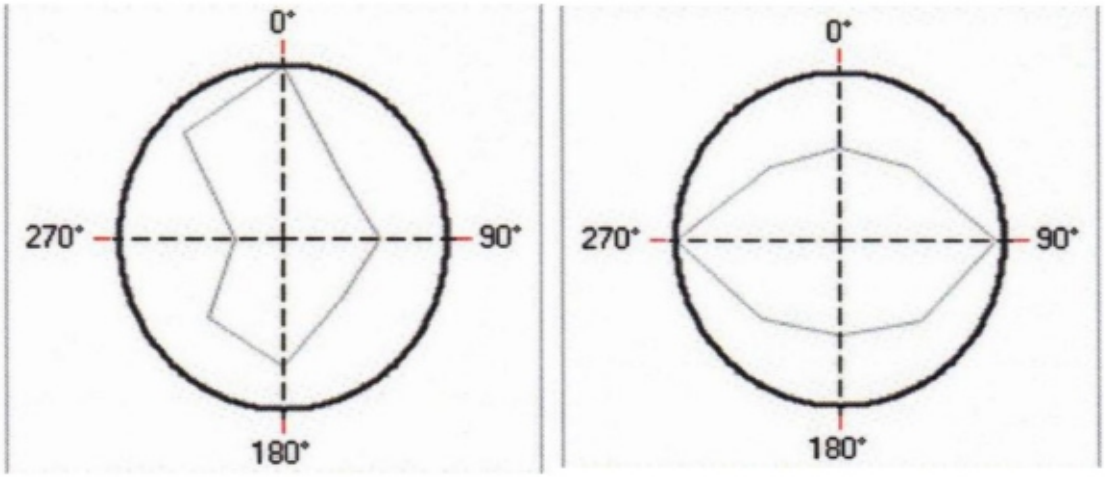

Figure 11: Category 1&Category 0 response

CONCLUSION

In this paper it was shown that the application of focus response guided wave technique for corrosion detection. With this specific technique it is availbale to get more information from suspected area in term of how localized the ultrasonic response around circumference for very close severity estimation of each corrosion defects.Although Guided Wave method is known as a monitoring system and will shows the cross-sectional change of features, by Using Focus Response evaluation Technique, dimention of each corrosion defects will achive.The most important benefit of guided wave is 100% coverage and screening for corrosion. This complements conventional NDT, which aims to detect and evaluate flaws in specific critical areas. These areas are often inaccessible, and can be dangerous for test operators, but could be reached by guided waves.

REFERENCES

[1] P. Cawley, D.N. Alleyne, B. Pavlakovic, and M.J.S. Lowe "THE USE OF GUIDED WAVES FOR RAPID SCREENING OF PIPEWORK". Dept Mechanic Eng, Imperial College, London, UK Guided Ultrasonics Ltd, Nottingham, UK

[2] M.J.S. Lowe and P. Cawley "Long Range Guided Wave Inspection Usage – Current Commercial Capabilities and Research Directions" Department of Mechanical Engineering Imperial College London, 29 March 2006

[3] Jing Mu, Li Zhang, Joseph L. Rose and Jack Spanner "DEFECT SIZING IN PIPE USING AN ULTRASONIC GUIDED WAVE FOCUSING TECHNIQUE" Department of Engineering Science and

Mechanics, The Pennsylvania State University, University Park,
[4] Graham EDWARDS "Long Range Ultrasonic Testing – New Markets for New Technology" Document: LRUCM/LON/TWI/GE/010806/1 –TWI Ltd
[5] K. Worden, C. R. Farrar, G. Manson, and G. Park, "The fundamental axioms of structural health monitoring," Proc. R. Soc. A Math. Phys. Eng. Sci., vol. 463, no. 2082, pp. 1639–1664,Jun. 2007.
[6] T. Clarke, F. Simonetti, and P. Cawley, "Guided wave health monitoring of complex structures by sparse array systems: Influence of temperature changes on performance," J. Sound Vib., vol.329, no. 12, pp. 2306–2322, Jun. 2010.

ISSN 2320-2092

TURBOCHARGER DESIGN CRITERIA, SELECTION AND FAILURE

RAJVARDHAN NALAWADE
UNDERGRADUATE, COLLEGE OF ENGINEERING PUNE, WELLESLEY ROAD, SHIVAJINAGAR, PUNE-05

A B S T R A C T

This paper presents step by step design procedure and considerations while matching a turbocharger to a specific engine. One simple and efficient way of matching a turbocharger to an engine is the "Ballpark Matching" technique. Turbochargers are the most efficient horsepower supplementing unit in a vehicle, and its installation requires changing certain components of an engine, and sometimes even installing completely new parts in the engine, like aftercoolers. For heavy duty purposes where it is targeted to increase the horsepower by more than 50%, we have to do certain changes in the crankshaft, piston and other parts of an engine. Once a turbocharger is selected and installed, the next step is tuning the turbocharger according to the fuel injection characteristics and extracting maximum out of the turbocharger. The last and most important phase is the failure analysis and detection in a turbocharger. Certain typical turbocharger failures will be discussed along with troubleshooting.

Indexterms - *Turbocharger Matching, Tuning, Compressor, Wastegates, Anti Lag Systems*

I. INTRODUCTION

A turbocharger works on the basic principle of extracting air from exhaust and directing it to rotate the turbine. This rotation of the turbine leads to rotation of the shaft on which the turbine and turbine housing is mounted. This rotation of the shaft causes the compressor wheel on the other side to rotate. This compressor, compresses the static air present around it thus, increasing the number of air molecules per unit volume. This dense air is pumped inside the engine, Hence, in this way the volumetric efficiencyof the engine will increase. Volumetric efficiency is the volumetric flow rate of air versus the capability or theoretical flow rate possible.

A 100% volumetric efficient engine is not possible, because of many reasons like installation of air filter, etc. Small increments can be made in the volumetric efficiency can be made by increasing the valve open times, and increasing their sizes. However, if dense and more air is pumped into the engine, its volumetric efficiency will drastically increase. The types of installation of turbos are of three types, namely single turbos, twin turbos or series turbos.In twin turbos, two turbos give the input to an engine. Whereas, in series turbos, the output of one compressor is fed to the second turbine. This leads to high level of compressing and used in heavy duty operations like tractors and cranes. In case of passenger vehicles with inline cylinder arrangement, single turbochargers are preferred. Whereas in case of V engines, twin turbochargers are preferred. In today's world, wastegates and variable geometry turbochargers are being widely used. A wastegate is nothing but a valve which opens to relieve excess exhaust gases. If the exhaust gas pressure is too much for the current speed of the vehicle, then an input is given to the wastegate from the compressor, which leads to opening of the wastegate and diverting a portion of the exhaust flow. This prevents the turbo from overcharging and thereby choking. It is the simplest application of a variable geometry turbine.

II. PARTS OF A TURBOCHARGER AND FUNCTIONING

The main parts of a turbocharger system are turbine, compressor, bearings and intercooler. The function of a compressor is to compress the air present in the volute portion of the compressor cover. Air flows through the bellmouth nozzle along the inducer diameter. This diameter of the inducer decides the flow rate or capacity of the compressor. The diffuser portion of a compressor is very vital as it governs the flow of the air from the compressor to the cover. The compressor and cover have a gap of nearly 0.01 inch. Most diffusers are vaneless type and are formed by parallel walls between cover and bearing housing face. The vane type diffuser, being restrictive is only used in engines with a very narrow RPM operating range. The volute diameter increases as it gradually approaches he engine as it has to convert the highly dense moving air into static pressure air. At times, an inducer bleed is installed before the inlet of the compressor, which diverts excess flow and allows its re-entry into the compressor. This prevents compressor from surging. The range of operating and maximum efficiency RPM for a compressor with a particular A/R (area over radius) ratio can be found by plotting its pressure ratio against air flow compressor map. Some compressor types are straight radial, backward curved impellor and splitter blade type.

The next vital component is the turbine which is rotated by the exhaust air moving through the turbine housing tongue. Turbine shafts are manufactured by rolling to keep intact the grain structure of parent metal. There are two basic types of turbine, namely, tangential entry and divided type. A divided type allows the air to reach the turbine tip and lets out a collective uniform stream of air. However, the tangential entry type is less restrictive and delivers output in form of exhaust pulses. Turbine sizing is also done by A/R ratio. It is the area of the volute divided by the radius from center to the volute centroid.

Bearing system consists of two journal bearings and a flat thrust bearing. This has now been replaced by ball bearings. Ball bearings, when installed give a better initial response than the journal bearings.

III. SELECTING A TURBOCHARGER

The method of selecting a turbocharger is called the “Turbocharger matching” technique. In this, we have to first match the compressor and then the turbine. Depending upon the capacity of the engine, the displacement of the engine is used to calculate the airflow.

$$\text{Airflow} = \frac{\text{Displacement} \times \text{RPM}}{2}$$

With this, the airflow is found out and is multiplied by a factor of 0.85, so as to compensate the various losses contributing to the volumetric efficiency. The amount of boost pressure is decided and a ratio called pressure ratio is defined as

$$\text{Pressure ratio} = \frac{\text{Boost pressure} + \text{Surrounding Pressure}}{\text{Surrounding pressure}}$$

The pressure ratio against density ratio graphs are used to find the corresponding density ratio. This density ratio, when multiplied with the corrected airflow, it gives us the turbocharged airflow. With these data in hand, we refer to air flow versus pressure ratio graphs of several compressors and see which compressor gives us the best results for the given data. The central regions of such compressor maps usually represent the highest efficiency island. The trim of a compressor determines the capacity of the compressor to handle large airflows.

$$\text{Trim} = \frac{\text{Inducer} \times \text{Inducer}}{\text{Exducer} \times \text{Exducer}} \times 100$$

In case of turbines, pressure ratio is replaced by the term called expansion ratio. It is the reverse of pressure ratio

$$\text{Expansion ratio} = \frac{\text{Exhaust Pressure} + \text{Atmospheric Pressure}}{\text{Turbine Pressure} + \text{Atmospheric Pressure}}$$

Now, using a turbine flow map which has corrected flow on Y axis and expansion ratio on X axis, we can find the corresponding corrected flow rate. Based on this flow rate and the size of the turbine or the A/R ratio, we can choose the appropriate turbine. A small A/R ratio shows increase in exhaust pressure. Two turbines having the same A/R ratio need not have the same volumetric efficiency due to difference in the velocity of the exhaust air inside the turbine housing. The exhaust air velocity depends on the radius of the housing. It varies inversely with the radius, to be more specific. Hence, turbines having same A/R ratio have similar turbine maps, however their magnification differs. It is important to test the turbine pressure while installing a turbine on an engine. Hence, a pressure tap must be fitted in the turbine for testing purpose to check that the pressure of the turbine does not vary drastically with respect to compressor.

IV. DESIGN CONSIDERATIONS OF TURBOCHARGER AND ENGINE

The design of a turbocharger begins with the decision, should the turbocharger be two twin turbochargers or 1 large single turbocharger. Logically, when the size of a turbocharger increases the moment of inertia increases. Hence, as the moment of inertia increases, the resistance to the rotatory parts of a turbocharger increases. If we take two small turbochargers and arrange them in parallel, the resultant moment of inertia is clearly, less than that of a large single turbocharger. However, there is a disadvantage to twin turbocharger system too. As there are two turbochargers involved, it means there will be frictional losses in the clearance between turbine housing and turbine in two turbochargers. Therefore, more losses and less efficiency is a result. Twin turbochargers should only be used in large applications.

Intake filters of a turbocharger system have to be less restrictive as compared to general intake air filters of vehicles, made of filter paper. A fine filter will clog too many particles, thus causing a high pressure drop and choking the turbocharger. Instead, a filter made of surgical gauze must be used, which will be less restrictive. If a K&N filter is to be used, we can use the following formulae provided by K&N to determine filter characteristics

$$\text{Area(sq inch) of filter} = \left\{\frac{\text{lbs of boost}}{14.7} + 1\right\} \times \text{Cubic Inch Displacement} \times \text{RPM} \div 20839$$

$$\text{Filter height(inch)} = \frac{\text{sq inch of filter}}{\text{filter diameter} \times 3.14} + 0.75$$

If we decide the boost pressure beyond 5-7lbs, an aftercooler is a must. According to the Ideal Gas Equation

$$PV = nRT$$

We know that as the pressure of the air inside compressor increases, the temperature will increase. Hence intercoolers are required. Efficiency of an intercooler can be found out by

$$\text{Efficency} = \frac{\text{Compressor} - \text{Intercooler}}{\text{Compressor} - \text{Surrounding}} \text{Temperatures}$$

The intercooler may be of shell and tube type or cross flow heat exchanger, depending upon the application.Worm clamps must be used for tightening of hoses as they are easy to tighten and have high resistance to wear. One end of the turbocharger is connected to the plenum and the other end to the exhaust manifold. Flex tubes and expansion joints must be used throughout to increase durability and increase the ability to withstand temperature. Ceramic paint acts as a good heat shield for the turbocharger.

If we are aiming to boost an engine above 50% of original power, we need to make certain changes in the engine. The engine block is put through the following processes. First, the block is heated for 30 minutes up to 500 degree Fahrenheit. Next, it is bead blasted and shaken well to remove debris. Magnaflux test is performed to test for cracks and then, a sonic check is done to see the thickness of the block and itsvariation. Lastly, honing plates are installed in the bore of the engine block and its reading is taken when the block head is installed and bolted. If the reading is large enough, then it leads to buckling during operation. Crankshafts must be forged and not cast. Cast components often have pores in them leading to loss in strength. A billet crankshaft, in which the whole crankshaft is made from a single block is even better. The crankshaft must be properly balanced on the main bearings. In case of pistons, the topmost piston ring is usually very close to the piston crown. This results in a very little area as a combustion dead spot between the topmost ring, piston crown and cylinder wall. However, this small are is responsible for leakage of air and fuel mixtures too. Hence, bringing the piston rings down is not possible. This affect the turbochargers performance. Heat treated, hypereutectic pistons with 12% silicon content are ideal for high horsepower turbocharger applications. Piston coatings like ceramic keep the piston cool and fasten the heat transfer rate, however decrease the clearances between piston and cylinder. Connecting rods must be preferably, of the H beam design as compared to the I beam, for better wear resistance. The connecting rod bolts must be large enough to withstand the new power and torque on it.

Valves must be modified such that they provide for higher airflow and hence speed up the process of combustion. The valve seat, if narrowed by grinding and polishing, will lead to higher airflow. In addition to this, it must be made sure that all the combustion chambers have the same volume. Gaskets must be used extensively and positive type head gasket such as O-rings must be used. Also, head studs are recommended.

The rate at which dense air will enter the engine combustion chamber will be very high than the rate of fuel injection. Hence, this needs a cam lobe profile change. Note that by grinding and polishing cam lobes, we cannot increase the time for which the cam is open by a large amount. More importantly, we cannot increase it, but can decrease it slightly. However, we can change the rise or lift at a particular cam position. This can be done by grinding and polishing the surface of the cam. A thick cam leads to high lifts or rises and a narrow cam profile leads to short rises. Make sure to round the edges to smoothen the transition. These small edits to an engine and the design considerations while installing a turbocharger

will keep the engine healthy and running for quite a long period of time.

V. TUNING A TURBOCHARGER

Tuning an engine can be best described as controlling the amount of air and fuel being injected in the combustion chamber at once. With the installation of a turbocharger, more air enters the combustion chamber than the stock values. Hence, to maintain the compression ratio, the fuel injected must be more as well. Sometimes, there is a need to change the fuel injectors as well.
The first step while tuning a turbocharged engine is the installation of an exhaust gas oxygen sensor after the exhaust header. The function of this sensor is to measure the air fuel ratio, also denoted by lambda λ. Next, the fuel injector duty cycle needs to be increased. Duty cycle is the amount of time for which the injectors are open, delivering fuel. Care must be taken that the duty cycle is not above 90% of the total time, and in such cases, fuel injectors must be replaced with larger ones. Injectors have to be chosen depending upon the brake specific fuel consumption of an engine. Generally, the turbocharged engines have a brake specific fuel consumption of 0.60. Injector ideal size can be found out by

$$\text{Size} = \frac{\text{Horsepower} \times \text{BFSC}}{\text{Number of injectors} \times \text{Duty cycle}}$$

Fuel pressure in the rails is related directly to the square of the mass flow rate of an injector. Keeping these formulae in mind, the ideal injector for a turbocharged engine can be tuned and chosen.
Blow off valves and compressor valves have to be installed. In cases where the throttle is suddenly shut off, but the vehicle is in motion, the compressor is run due to exhaust being emitted. However, there develops too much backpressure in the engine due to zero throttle condition and this leads to wear of the turbocharger. This unwanted air in the compressor can be let out using a blow off valve. This valve is actuated when the throttle is deactivated and then it diverts the exhaust flow out into the atmosphere. In case of compressor valves, they divert the exhaust flow back into the intake of an engine. This clearly suggests that blow off valves give a noisy output as compared to compressor valves.
In case of wastegate turbochargers, boost controllers are used to limit the boost generation with the help of a needle valve.
In extreme racing vehicles, we sometimes need immense horsepower the moment we start the race. In such cases it is demanded that the turbocharger be activated in the start as soon as the engine is switched on and idling. This has been achieved by Anti Lag Systems. When the throttle and clutch are pushed simultaneously, the ALS system gets activated and it misfires a cylinder, thus causing exhaust to rotate the turbine vigorously. This leads to violent firing inside the combustion chamber and leads to rapid rotation of the turbine. Although this leads to high temperatures in the turbocharger and the engine, it is used by racers to improve their pick up speed.

VI. FAILURE ANALYSIS

Turbocharger is a part of an engine that is subjected to extreme stresses, due to its extreme surrounding conditions and number of cycles of operation. Hence, the failure of a turbocharger is a common event, especially in drag races. A turbocharger rarely lasts for an entire season of a racing event. The analysis of failures in turbochargers is a field in itself. There are majorly, four main causes of turbocharger failure, namely: External damage, contaminated oil, lack of lubrication and high exhaust temperatures.

External damage may be found out by making some typical observations. The intercooler acts as a catch pot, in most cases. It prevents the entry of external particles into the compressor and hence protects the engine. However, bolts and rocks may be found in the compressor housing which show that the reason of failure is external object ingression. The particles which do not enter the engine, often get dislodged into the turbine housing, thus deteriorating the performance. Valve and piston fragments, along with heat baffle fragments may be found in the turbine housing, leading to failure. Rather than this, the risks of a turbine failing by over speeding are excessively high. Turbines cannot last over 100,000 cycles in general. The heat generated and the mass air flow cannot be sustained after a limit and the turbine blades start chipping off, thus affecting performance.

Contaminated lube oil leave markings on the journal bearing. Marks can be seen, predominantly on the outer diameter of the bearings, due to trapped particles. If contaminated oil is the only cause of failure, scoring can be seen on the internal diameters of the bearings too, to an extent. Contaminants in the oil gallery and poor oil filter maintenance leads to contaminated lube oil.

Discoloration in the thrust and journal bearings, show a clear case of lack of lubrication. The first run of a turbocharger is without the oil lubrication. This is a cause for failure. Any sludge in the bearing housing that blocks the oil or damaged oil line, lead to failures due to lack of lubrication. When oil is found in both the ends of housing, it means that there has been oil leakage. This happens due to broken piston rings or an improper placement of oil drain.

The turbocharger bearing assembly is in continuous motion. When the boost pressure acts on the back of compressor, the thrust bearing is pulled farthest away towards the positive side. Hence, the bearing system may fail after many cycles of sudden acceleration and deceleration. In case of drag races, there is always a negative pressure differential generated across the ends as the compressor will never be able to cope up with the requirements of a turbine. Once we, move up to the next gear, the boost pressure slowly overcomes the turbine pressure. This shows that in races, the bearings are in constant motion and may fail soon if not lubricated well.

CONCLUSION

These are the basic design considerations that every individual needs to be familiar with before installing a turbocharger to an engine. The steps to do this are as follows: Selecting the appropriate turbocharger, designing the turbocharger parts, changing the engine according to the requirements and finally, tuning the turbocharger.

REFERENCES

[1] Corky Bell, "Maximum Boost: Designing, Testing and Installing Turbocharger Systems"
[2] Hugh MacInnes "How to Select and Install Turbo-chargers"
[3] Roland Merkle, Wolfgang Rapp, Friedrich Noltemeyer "Installation of an exhaust gas turbo-charger at an internal combustion engine"
[4] Jeff Hartman, "How to Tune and Modify Automotive Engine Management Systems"
[5] Todd Curless, "Turbochargers: Theory, Installation, Maintenance, and Repair"

ISSN 2320-2092

ENGINEERING PROPERTIES OF CONCRETE MADE WITH PULVERISED FLY ASH

JONATHAN OTI
School of Engineering, Faculty of Computing, Engineering and Science, University of South Wales,Pontypridd, CF37 1DL, UK

ABSTRACT

This research work reports the potential of using Pulverised Fuel Ash (PFA) as a partial substitute for Portland Cement (PC) in the development of concrete. PFA is a by-product of the combustion of pulverized coal in electric power generating plants. Its use in concrete will alleviate the environmental concern for PFA disposal and ease the growing shortage and increasingly high cost of PC. In order to investigate the cement replacement potential of PFA, six types of mixes, at varying PFA replacement levels were designed— 5%, 10%, 15%, 20%, 25% and 30%; all with a water binding ratio of 0.6 and tested at 7, 14, and 28 days. The testing programme included material characterization; the determination of slump value and compressive strength. The results showed that the addition of PFA to the concrete mix causes the compressive strength to reduce at early age and that the slump values increased as the quantity of PFA increased in the mix.

Index Terms - *Pulverised Fuel Ash, Slump, Concrete, Compressive Strength*

I. INTRODUCTION

Due to the increasing demand for environmentally friendly and low cost construction materials;by-products from power plants and steel production are now being utilised as cement replacement materials in the construction industry. An example of such a material, is Pulverised Fuel Ash (PFA), which is a by-product of coal combustion from power plantsand is currently being stock-piled in open field landfill sites; thus having a negative impact on the environment. PFA has similar properties to Portland Cement (PC) owing to the available calcium content (CaO) [1] and so has the potential to be used as pozzolan for the partial replacement of cement. Replacing PC in concrete with PFA, will reduce thepollutant emissions, such as Carbon Dioxide and Nitrogen Oxide that are given off in the production of PC; thus helping to reduce greenhouse gases [2]. There have been a number of reports of the use of PFA in concrete.

Motamedi et al [3] reported that if the percentage of PFA used in PC replacement exceeds 20% of the total weight, the final UCS decreases. Openshaw [4] andSnelson et al [5] reported the same UCS reduction when the PFA content exceeds an optimum amount. Maslehuddin [6] carried out investigations to evaluate the compressive strength, development and corrosion-resisting characteristics of concrete mixes in which PFA was used as an admixture and from the results concluded that addition of Fly Ash as an admixture, increases the early age compressive strength and long-term corrosion-resisting characteristics of concrete. The superior performance of these mixes compared to plain concrete mixes was attributed to the increase in densification of the paste

structure which is a result of the pozzolanic action between the Fly Ash and the calcium hydroxide that is

from the hydration of cement. Jiang and Malhotra [7] tested Fly Ash of several different compositions, at 55% replacement. They demonstrated a strong positive correlation between lime content and compressive strength at all ages, although more notably at later ages.

This research reports on the results of the investigation on the slump value and strength of concrete made by the partial replacement of up to 30% of the PC in conventional concrete with PFA. The use of a cement replacement material such PFA in the production of concrete will increase environmental sustainability, by the reducing the high energy usage and carbon dioxide emissions that occur during cement production process. The paper will have a high impact on the Engineering and Scientific communities involved in alternative construction material development. The future impacts of this paper are for international development, through the development of techniques that will be transferable.

II. MATERIALS

A. Pulverised Fuel Ash

The Pulverised Fuel Ash (PFA) used within this research work was supplied by a local contractor and its manufacture conformed to BS EN 450-1 [8]. PFA is a by-product from coal-fired powered stations and is produced when pulverised coal is fed into the boilersand burnt at very high temperatures. The chemical composition and certain physical properties of PFA can be seen in Table 1.

Table 1 - Chemical composition and some physical properties of PFA

Chemical constituent PFA	Percentage
Silicon dioxide (SiO_2)	59·04
Aluminium oxide (Al_2O_3)	34·08
Iron oxide (Fe_2O_3)	2·0
Lime (CaO)	0·22
Sulphur trioxide (SO_3)	0·05
Magnesium oxide (MgO)	0·43
Alkalis (Na_2O, K_2O)	1·26
Loss on ignition	0·63
Characteristic of PFA	**Test result**
Lime reactivity; average compressive strength (MPa)	6·59
Specific gravity	2·058
Fineness: specific surface area (m^2/N)	35·48
Drying shrinkage (mm)	0·06
Soundness by autoclave test expansion of specimen (mm)	0·01

B. Portland Cement

The Portland Cement (PC) used throughout this research was manufactured in accordance with BS 197-1 [9] and supplied by Lafarge Cement UK. The minimum compressive strength of the PC is 32.5 N/mm2. The physical properties and Oxide/chemical composition of the PC are shown in Table 2.

Table 2 - Physical properties and Oxide/chemical composition the PC

Properties	
Insoluble Residue	0.5
Bulk Density (kg/m³)	1400
Relative Density	3.1
Blaine fineness (m^2/kg)	365
Colour	Grey
Oxide	**%**
SiO_2	20.00
Al_2O_3	6.00
Fe_2O_3	3.00
MgO	4.21
MnO	0.03 - 1.11
SO_3	2.30
Loss on Ignition	0.8
Chemical (%)	
Cl	0.03
Free lime	1.32
Bogue's composition	
Tricalcium aluminate (C_3A)	6.48
Tricalcium silicate (C_3S)	70.58
Dicalcium silicate (C_2S)	6.09
Tetracalcium alumunate-ferrite (C_4AF)	6.45

C. Limestone Aggregates

The limestone aggregate used throughout this investigation were sizes 10mm and 20mm. The limestone aggregates were supplied by a local quarry and complied with the requirements of BS EN 12620 [11]. Some geometrical, mechanical and physical properties of the limestone aggregate can be seen in Oti and Kinuthia [10].

D. Sand

The sand used throughout this study was natural sea-dredged sand from the Bristol Channel. Some geometrical, mechanical and physical properties of the sand can be seen in Oti and Kinuthia [10]. The sieve analysis of the sand was performed in accordance with BS EN 933-1: [12] and the results are given in Table 3.

Table 3 - Sieve analysis of the limestone aggregate and sand

Sieve Sizs (mm)	Sand	Limestone 10/4.
31.5	100	100
16	100	100
8	100	77
4	100	2
2	83	0.3
1	54	0.28
0.5	21.8	0.19
0.25	6	0.14
0.125	1.2	0.1

III. METHODOLOGY

The control mix for the concrete in the current research work was designed using a PC content of 374 kg/m3. The water/binder ratio was 0.5, with a slump value of 7mm. In order to investigate the cement replacement potential of Fly Ash, the investigation used up to 30% Fly Ash to replace the PC in the control mix, in various combinations as shown in Table 4. The intention is to maintain a specified consistency but to obtain usable concrete, irrespective of consistency, using Fly Ash and, if possible, without using superplasticisers, which is more cost-effective. The first mix to be referred to as JO1, is the control mix. For the second mix (Jo2), the PC in the control concrete was be replaced with 5% Fly Ash. In the third mix (Jo3), the PC in the control concrete was be replaced with 10% Fly Ash. For the forth mix (Jo4), the PC in the control concrete was be replaced with 15% Fly Ash. In the fifth mix (Jo5), the PC in the control concrete was be replaced with 20% Fly Ash. For the sixth mix (Jo6), the PC in the control concretewas replaced with 25% Fly Ash. The final mix (Jo7),was produced by replacing the PC in the control concrete with 30% Fly Ash.

Table 4 - The mix composition

Mix Code	Binder (kg)		Coarse Aggregate (kg)		Sand (kg)	Water (kg)
	PC	PFA	20./10	10./4		
JO1 (Control)	5.69	0	11.94	5.12	11.52	2.97
JO2	5.40	0.29	11.94	5.12	11.52	2.97
JO3	5.12	0.59	11.94	5.12	11.52	2.97
JO4	4.84	0.85	11.94	5.12	11.52	2.97
JO5	4.55	1.14	11.94	5.12	11.52	2.97
JO6	4.27	1.42	11.94	5.12	11.52	2.97
JO7	3.98	1.71	11.94	5.12	11.52	2.97

Cube (100 mm × 100 mm × 100 mm) test specimens were used in the production of all the concrete. For all mix compositions, the test specimens, were prepared in accordance with BS EN 206 [13], BS EN 12350-1[14] and BS EN 12390-1 [15]. The consistency of the fresh concrete was measured using slump test in accordance with BS EN 12350-2 [16]. De-moulding of the test specimens was done after 24 hours. The curing of the test specimens were carried out in accordance with BS EN 12390-2 [17]. All the cube specimens were tested for 7, 14 and 28 day compressive strength in accordance with BS EN 12390-3 [18] and BS EN 12390-4 [19]. For all mix compositions, the results reported are the average obtained from five individual specimens for compressive strength.

RESULTS

The results for the slump for each of the mixes are presented in Figure 1. It can be seen that the more PFA there is in the mix, the higher the slump value, suggesting that more PFA gives a wetter mix.
The slump values varies from 7mm slump for mix Jo1 with no PFA in the mix, to 50mm for JO7; giving an early indication as to the behaviour of the concrete in a fresh state. The trend is relatively constant throughout the range of mixes, however, two anomaly points were observed. Mix JO4 shows a lower slump from the linear trend-line of the other mixes; as does Jo7, which shows no increase in slump value compared to JO5, even though additional 5% PFA was added to the mix

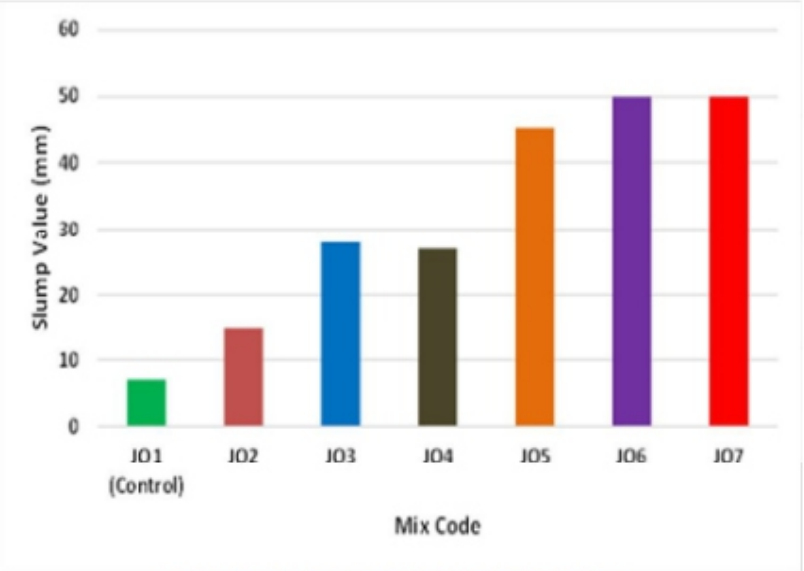

Figure 1 - Slump value for all mixes

Figure 2 shows the results of the compressive strength test for 7, 14 and 28 days. There was a progressive increase in strength values for all the mix compositions with age. The highest 7 day strength observed was, JO1 which was the control mix; while the lowest strength was observed for mix JO7, wherePC in the control mix was replaced by 30% PFA. Increasing the PFA content of a concrete mix caused a reduction in compressive strength in early age.

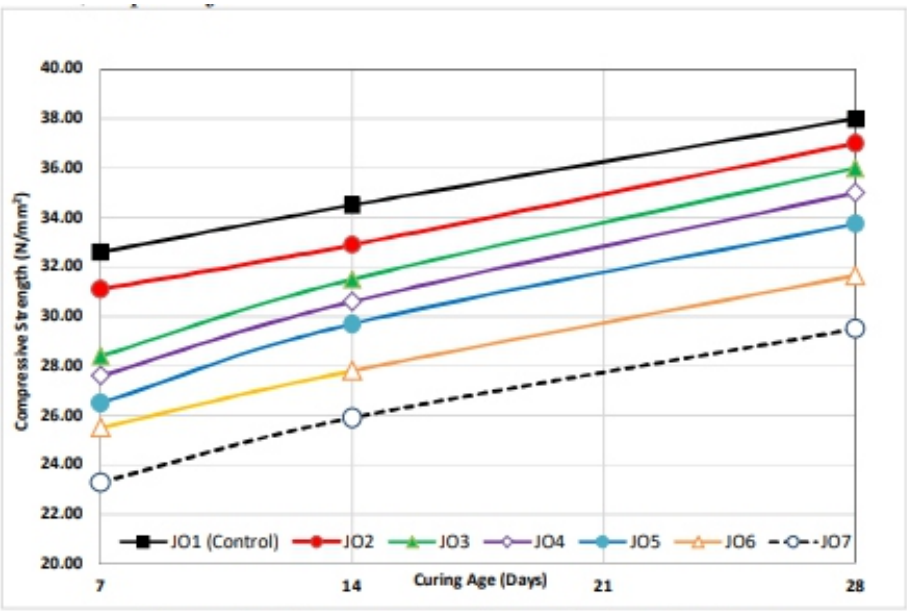

Figure 2 - Compressive Strength for all mixes

DISCUSSION

There were some observed variations in the slump values of the various mixes with the addition of PFA. A continual trend of increasing slump values developed for every percentage increase in the amount of PFA in the concrete mix, except in mixes JO4 and JO7. In compliance with BS EN 12350 [16], the seven mixes produced can be categorised, resulting in Jo1 being not classified (i.e. below 10mm), JO2 to JO4 being classed as S1 and JO5 to JO7 being classed as S2. The increase in slump values with PFA addition may be attributed to the extremely spherical particle shape of PFA which may act as miniature ball bearings within the concrete mix, thus providing a lubricant effect [10]. Using the PFA would make the consistency of the concrete mixes flow more easily on site and so speed up the construction process. Mixes JO6 and JO7 had the largest slump values making the concrete wetter. These mixes also had the highest PFA content asthe water content was identical in all mixes. The results showed that PFA can be used not only as a cement replacement material but also as a substitute for water content.

The variations observed with regards to the compressive strength were a progressive increase in strength values for each mix composition, as the curing age increased. Mix JO1, the control mix,attained a higher strength at 28 days. This higher strength gain may be due to the gradual formation of the calcium silicate hydrate gel (C-S-H gel) in the hydration process. The more PFA in the mix, the lower the overall strength of the mix. PFA was found to have an increased effect on concrete strength development at later age. To further understand the long term effect of adding PFA to concrete, it is necessary to test the strength at later age (beyond 28 days).

CONCLUSIONS

The investigation carried out in the current study has demonstrated the potential of replacing up to 30% of PC with PFA. The key conclusions that can be drawn from this investigation are summarised in the following list:

1) There was variation in the slump values of the concrete mixes with the addition of PFA. The lowest slump value was observed from the control mix while the highest slump value was observed from mixes JO6 and JO7, these are the mixes where 25% and 30% of the PC in the control mix was replaced with PFA.
2) The results of the compressive strength test showed that the highest strength value was obtained for the control mix while lowest strength was obtained from the concrete where 30% of the PC in the control concrete was replaced with PFA.

REFERENCES

[1] S Motamedi, K Song, R Hashim., 2015. Prediction of unconfined compressive strength of pulverized fuel ash–cement–sand mixture, Mater. Struct. 48 (4) (2015) 1061–1073.
[2] Sivakumar, M. & Manikandan, T., 2014. An Experimental Study on Strength Development of Concrete Containing Composite Ash (Flay Ash-F & Rice Husk Ash). InternationalJournal of Engineering Research & Technology (IJERT), 3(4), p. 1140
[3] S. Motamedi, K.-I. Song, R. Hashim., 2015. Prediction of unconfined compressive strength of pulverized fuel ash–cement–sand mixture Mater. Struct., 48 (4), pp. 1061-1073
[4] C. Adriano, A.L. Page, A.A. Elseewi, A.C. Chang, I. Straughan., 1980. Utilization and disposal of fly ash and other coal residues in terrestrial ecosystems: A review J. Environ. Qual., 9 (3) (1980), pp. 333-344
[5] D.G. Snelson, J.M. Kinuthia, P.A. Davies, S.-R. Chang. 2009. Sustainable construction: Composite use of tyres and ash in concrete Waste Manag, 29 (1), pp. 360-367
[6] Maslehuddin, M (1989) Effect of sand replacement on the early-age strength gain and long-term corrosion-resisting characteristics of fly ash concrete, ACI, page 58-62.
[7] L Jiang and V Malhotra. Reduction in water demand of non-air-entrained concrete incorporating high volumes of fly ash. Cement and Concrete Research, 2000, 30, No. 11, pp1785–1789.
[8] BS EN 450-1:2012. Fly ash for concrete – Part 1: Definition, specifications and conformity criteria.
[9] BS EN 197-1: 2011. Cement - Part 1: Composition, Specification and Conformity Criteria for Common Cements.
[10] Oti J.E and Kinuthia JM., 2016. Engineering Properties of Concrete made with Brick Dust Waste. In the Proceedings of the 9th International Concrete Conference in Dundee, Jones MR, Newlands MD, Halliday JE, Csetenyi LJ, Zheng L, McCarthy MJ, Dyer T., 2016 (eds), Pg. 69-77.
[11] BS EN 12620:2002 +A1:2008. Aggregates for concrete
[12] BS EN 933-1:2012-Tests for geometrical properties of aggregates Part 1: Determination of particle size distribution —Sieving method
[13] BS EN 206:2013-Concrete. Specification, performance, production and conformity
[14] BS EN 12350-1:2009. Testing fresh concrete Part 1: Sampling.
[15] BS EN 12390-1:2009.Testing hardened Concrete. Part 1: Shape, dimensions and other requirements of specimens and moulds
[16] BS EN 12350-2:2009. Testing fresh concrete Part 2: Slump-test.
[17] BS EN 12390-2:2009.Testing hardened Concrete. Part 2: Making and curing specimens for strength tests.
[18] BS EN 12390-3:2009.Testing hardened Concrete. Part 3: Compressive strength of test specimens.
[19] BS EN 12390-4:2009.Testing hardened Concrete. Part 4: Compressive strength - Specification for testing machines.

Instructions for Authors

Essentials for Publishing in this Journal

1 Submitted articles should not have been previously published or be currently under consideration for publication elsewhere.

2 Conference papers may only be submitted if the paper has been completely re-written (taken to mean more than 50%) and the author has cleared any necessary permission with the copyright owner if it has been previously copyrighted.

3 All our articles are refereed through a double-blind process.

4 All authors must declare they have read and agreed to the content of the submitted article and must sign a declaration correspond to the originality of the article.

Submission Process

All articles for this journal must be submitted using our online submissions system. http://enrichedpub.com/ . Please use the Submit Your Article link in the Author Service area.

Manuscript Guidelines

The instructions to authors about the article preparation for publication in the Manuscripts are submitted online, through the e-Ur (Electronic editing) system, developed by **Enriched Publications Pvt. Ltd**. The article should contain the abstract with keywords, introduction, body, conclusion, references and the summary in English language (without heading and subheading enumeration). The article length should not exceed 16 pages of A4 paper format.

Title

The title should be informative. It is in both Journal's and author's best interest to use terms suitable. For indexing and word search. If there are no such terms in the title, the author is strongly advised to add a subtitle. The title should be given in English as well. The titles precede the abstract and the summary in an appropriate language.

Letterhead Title

The letterhead title is given at a top of each page for easier identification of article copies in an Electronic form in particular. It contains the author's surname and first name initial .article title, journal title and collation (year, volume, and issue, first and last page). The journal and article titles can be given in a shortened form.

Author's Name

Full name(s) of author(s) should be used. It is advisable to give the middle initial. Names are given in their original form.

Contact Details

The postal address or the e-mail address of the author (usually of the first one if there are more Authors) is given in the footnote at the bottom of the first page.

Type of Articles

Classification of articles is a duty of the editorial staff and is of special importance. Referees and the members of the editorial staff, or section editors, can propose a category, but the editor-in-chief has the sole responsibility for their classification. Journal articles are classified as follows:

Scientific articles:

1. Original scientific paper (giving the previously unpublished results of the author's own research based on management methods).

2. Survey paper (giving an original, detailed and critical view of a research problem or an area to which the author has made a contribution visible through his self-citation);

3. Short or preliminary communication (original management paper of full format but of a smaller extent or of a preliminary character);

4. Scientific critique or forum (discussion on a particular scientific topic, based exclusively on management argumentation) and commentaries. Exceptionally, in particular areas, a scientific paper in the Journal can be in a form of a monograph or a critical edition of scientific data (historical, archival, lexicographic, bibliographic, data survey, etc.) which were unknown or hardly accessible for scientific research.

Professional articles:

1. Professional paper (contribution offering experience useful for improvement of professional practice but not necessarily based on scientific methods);
2. Informative contribution (editorial, commentary, etc.);
3. Review (of a book, software, case study, scientific event, etc.)

Language

The article should be in English. The grammar and style of the article should be of good quality. The systematized text should be without abbreviations (except standard ones). All measurements must be in SI units. The sequence of formulae is denoted in Arabic numerals in parentheses on the right-hand side.

Abstract and Summary

An abstract is a concise informative presentation of the article content for fast and accurate Evaluation of its relevance. It is both in the Editorial Office's and the author's best interest for an abstract to contain terms often used for indexing and article search. The abstract describes the purpose of the study and the methods, outlines the findings and state the conclusions. A 100- to 250-Word abstract should be placed between the title and the keywords with the body text to follow. Besides an abstract are advised to have a summary in English, at the end of the article, after the Reference list. The summary should be structured and long up to 1/10 of the article length (it is more extensive than the abstract).

Keywords

Keywords are terms or phrases showing adequately the article content for indexing and search purposes. They should be allocated heaving in mind widely accepted international sources (index, dictionary or thesaurus), such as the Web of Science keyword list for science in general. The higher their usage frequency is the better. Up to 10 keywords immediately follow the abstract and the summary, in respective languages.

Acknowledgements

The name and the number of the project or programmed within which the article was realized is given in a separate note at the bottom of the first page together with the name of the institution which financially supported the project or programmed.

Tables and Illustrations

All the captions should be in the original language as well as in English, together with the texts in illustrations if possible. Tables are typed in the same style as the text and are denoted by numerals at the top. Photographs and drawings, placed appropriately in the text, should be clear, precise and suitable for reproduction. Drawings should be created in Word or Corel.

Citation in the Text

Citation in the text must be uniform. When citing references in the text, use the reference number set in square brackets from the Reference list at the end of the article.

Footnotes

Footnotes are given at the bottom of the page with the text they refer to. They can contain less relevant details, additional explanations or used sources (e.g. scientific material, manuals). They cannot replace the cited literature.
The article should be accompanied with a cover letter with the information about the author(s): surname, middle initial, first name, and citizen personal number, rank, title, e-mail address, and affiliation address, home address including municipality, phone number in the office and at home (or a mobile phone number). The cover letter should state the type of the article and tell which illustrations are original and which are not.

Note